Chapter – 3

Experimental Investigation

3.1 General

Fluid flow characteristic around obstruction is important for natural and engineering point of view. In last few decades many research are carried out to find the flow behavior around hydraulic structures embedded in sand bed of the river or open channel. In case of river flow, the inclusion of sediments in the flowing water makes the analysis very complex. This water-sediment mixture exhibits a three dimensional, unsteady behavior and is subjected to turbulence. A lot of semi-empirical work as well as numerical techniques have been exploited in understanding these complex flows around structures in channel and still much is needed to get a full grip of the flow mechanism. Before the advent of computational fluid dynamics approaches, the direct field measurements and physical model studies of rivers with pier were conducted. However field measurements are not so simple and little work had been done on it. Therefore major focus was on experimental studies.

In the present study an attempt has been taken to find the flow characteristics and its influence on erodible channel bed around slender structures. To fulfill this purpose, a number of experimental programs are carried out in the Water Resources and Hydraulics Laboratory of the Department of Civil Engineering, Indian Institute of Technology (Banaras Hindu University), Varanasi, India

In this chapter, details description of experimental flume, measurement devices and experimental procedures are presented. The experimental model is developed keeping similarity with erodible sand channel bed in open channel flow. The pier structures in

physical system are modeled by simulation of cylindrical, rectangular and oval shape slender structures.

The maximum equilibrium scour depth around the piers model is observed in clear water flow conditions with erodible channel bed in flume. The effect of shape, size and fluid flow characteristics are experimentally studied for maximum equilibrium scour depth around these structures. Few studies are also carried out to observe the effectiveness of collar as a preventing device of scouring in erodible channel bed.

3.2 Description of Experimental flume

The experiments were conducted in a flume of 12m long, 0.43m wide and 0.53m deep channel in the Hydraulics Laboratory. The bottom of channel bed was made by steel and the side wall of the channel was made of perspex sheet throughout the length of the channel. Through the perspex sheet, the flow pattern around the pier model and scouring phenomenon in sand bed can be view from outside. The channel was open at the top just like an open channel. There was a slope altering device attached along with the channel bottom such that the slope can be altered as per our need. At the end of the channel a tail gate is provided to adjust the flow depth in the channel. There was a suitable mechanism to tilt the tail gate too. Water supplied through the pipe goes through such a mechanisms provided with the channel, that the flow should be as like open channel flow. The channel was constructed above the ground surface with the help of suitable mechanism. A photographical view of the setup is shown in the Figure 3.1 and schematic sketch is shown in Figure 3.2.

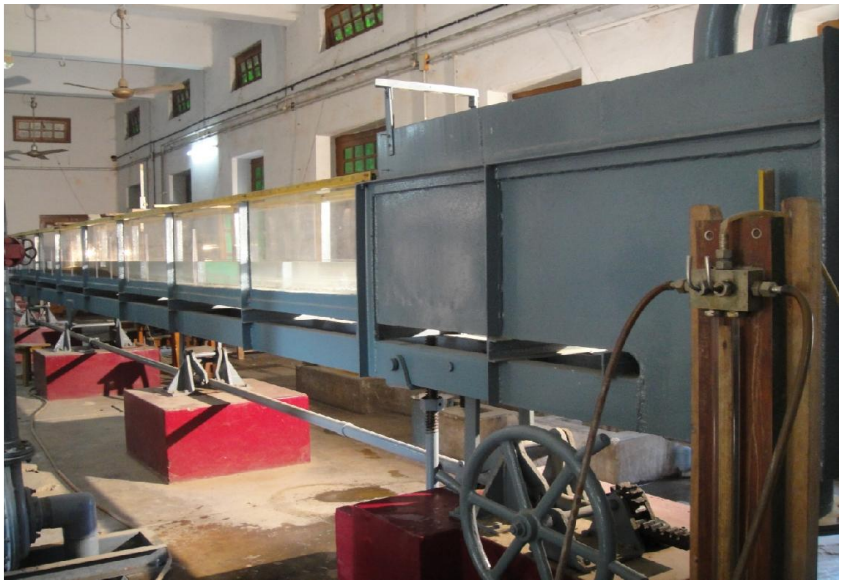

Figure 3.1: Photograph of Experimental Flume

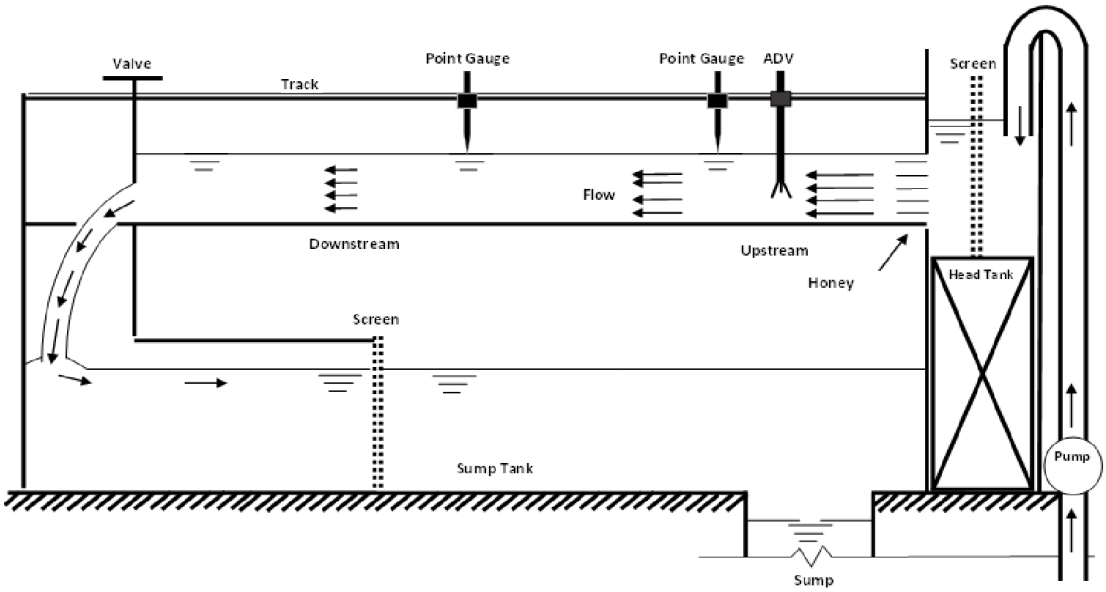

Figure 3.2: Schematic Sketch of Experimental setup

3.2.1 Flow Recirculating System

To conduct the experiments in the flume, large volume of water required for continuous flow in the channel section. Water was supplied into the channel from a sump tank constructed below the floor level of the laboratory. A 20 HP capacity centrifugal pump serves the purpose of lifting and supplying the water to the channel from sump. The water

supplied from tank crosses through the baffle wall, fitted inside the channel section, before entering the main stream of the channel to minimize the turbulence of flow. The flow can be controlled by the valve attached with the outlet pipe of the pump. The water after flowing into the channel stored in sump and re-circulates through the pump. The flow circulating system with centrifugal pump is shown in Figure 3.3.

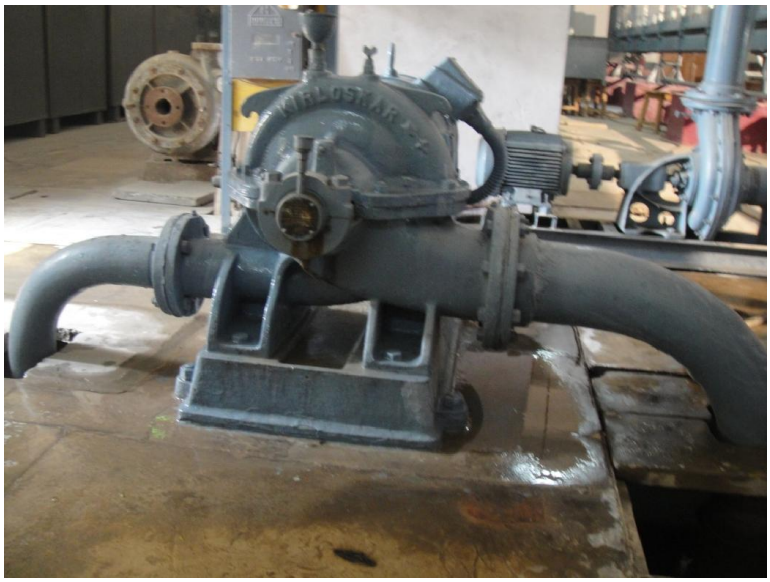

Figure 3.3: Flow recirculating system

The discharge and depth of flow in the channel was controlled by operating the discharge regulating valve fitted in the delivery pipe of the valve.

3.2.2 Measurement of Discharge and Depth of Water

Venturi Meter was used to measure the discharge in the flume indirectly. The Venturi Meter was connected in the delivery pipe of the pump which supplied the water in the head tank. The discharge was measured through the calibration curve corresponding to the height of mercury column of the Venturi Meter as shown in Figure 3.4.

Figure 3.4: Venturi Meter

An alternate discharge measurement device was in the downstream of the channel section. A rectangular notch was fitted in the downstream of the flume to measure discharge directly. Discharge was measured by using both devices to minimize the instrumental error. The depth of flow was measured from the bottom of the channel bed to free surface of the water.

A point gauge with a least count of 0.01cm was used to measure the water surface elevation above the bed of channel. The point gauge was installed in a moving platform. By this mechanism of moving platform, the instrument can measure the depth of flow at any point in the channel section along the length as well as width of the channel. The platform and point gauge used in the experiment work is shown in Figure 3.5.

Figure 3.5: Point gauge on sliding platform

The depth of flow in the channel section was also measured visually through the transparent scale pasted at the outside wall of the perspex sheet of the channel. The manual reading from the pasted scale and point gauge reading were measured each time to get accuracy in the measurement of depth of flow in the channel section.

3.2.3 Measurement of Flow Velocity and Direction

The flow characteristic in the channel section depends on flow velocity and its direction of flow. Measurement of flow velocity is very difficult at all point in the channel section. In the present experimental program, the point velocity in the flume was measured by 16-MHz Micro Acoustic Doppler Velocity meter (ADV) at few selected points only. The Micro-ADV uses the Doppler shift principle to measure the velocity of small particles, assuming to be moving at velocities similar to the fluid. Velocity is resolved into three orthogonal components (Tangential, radial and vertical) and measured in a depth below the sensor head. At every point, the instrument recorded a number of velocity data for a particular time (according to MHz). The mean value of the point velocities (three dimensional) were recorded for each flow depths.

Figure 3.6: Acoustic Doppler Velocity (ADV) setup

ADV was used to measure the 3-Dimensional velocity components. It is a remote sensing 3-D velocity sensor which transmits acoustic pulses into water, these pulses are then scattered by the particles present in water. The echo is received by the receivers of the ADV and the Doppler shift is calculated from the segments of the echo. The echo is Doppler shifted in proportion to the particle velocity. In the present study, 3-D down-looking probe were employed. The range of velocity that can be measured by this ADV is 1mm/s to 2.5 m/s and accuracy level is 1 % of measured range for sampling rate up to 50 Hz.

3.2.4 Preparation of flume bed

The channel bed was made up by steel and it was proper water proof. The side wall of the channel section was rigid one. To make the channel bed erodible as per real conditions, sand layer (Ganga River sand) was uniformly spread on the bottom of the channel. The distribution of particle size of the bed material is important parameters in study of scouring. Erosion of soil particle of the bed depends on the particle size and bed shear stress of flowing water. The physical characteristics of Ganga river sand was carried out in Geotechnical Laboratory. The tests result showed that the bed material consists of cohesion less sand with a median particle size (d_{50}) of 0.163 mm, specific

gravity of 2.59, coefficient of permeability of 1.01 x 10^{-3} cm/s, coefficient of uniformity (C_u) of 1.53, and coefficient of curvature (C_c) of 0.838.

A uniform sediment layer of 5 cm, 10 cm and 15cm thick is prepared and is spread along the length of the channel from 4.8 m to 7.3 m along the channel length. The sand is slightly compacted and leveled before conducting each experiment. To protect the excessive removal of sand particle a wooden barrier of small height was put downstream of the flume section. To begin, any experiments the bed is prepared properly and kept water standing on the bed for few minutes so that excessive erosion in transition stage can be minimized. The depth of water is measured from the top surface of the sand bed at initial level in steady state condition.

Figure 3.7: View of sand bed

3.3 Model of Slender Structure

To study the effect of slender structure in flow path of a channel section, different shapes and sizes of pier similar to slender structure is prepared in the laboratory. The material used for fabricating this pier was plane concrete and wood. Most of the bridge piers are in circular or oval shape, to simulate these cylindrical piers and oval piers are made and experiments are carried out. Rectangular shape piers are also fabricated to study extensively the flow behavior around slender structures.

The cylindrical, rectangular and oval pier those used in experimental program as a slender structure is shown in Figure 3.8, 3.9 and 3.10. The diameters of the piers are selected such a way that the effect of side wall is minimum interference in flow pattern. Many experimental model are fabricated few of them are mentioned here. Diameter of cylindrical shape piers are 2.25 cm, 3.18 cm, 3.86 cm and 4.38 cm. Characteristic diameter of rectangular piers are 3.38 x 3.04 cm, 4.15cm x 4.04 cm and oval shape piers are 2.9 x 1.5 cm, 4.7cm x 3.0 cm respectively.

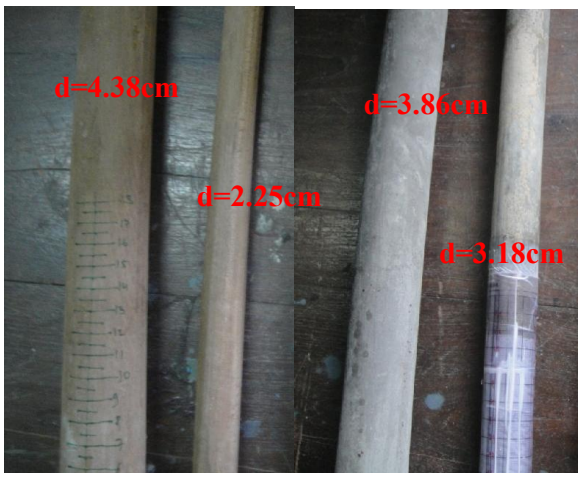

(a) Cylindrical shape model (b) Cylindrical model in flume

Figure 3.8: Cylindrical pier model

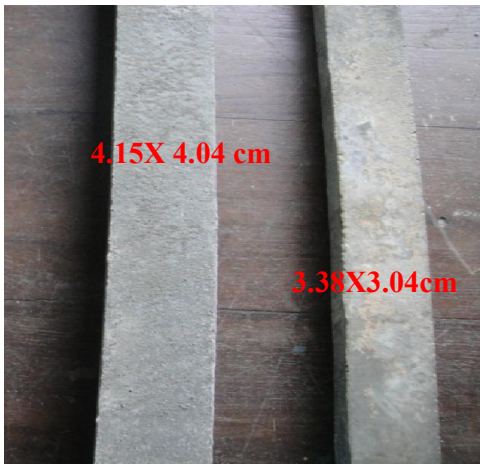

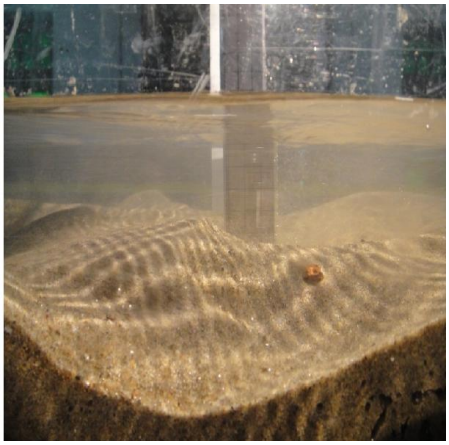

(a) Rectangular shape model (b) Rectangular model in flume

Figure 3.9: Rectangular pier model

(a) Oval shape model (b) Oval model in flume

Figure 3.10: Oval shape pier

3.4 Brief description of Experimental Procedures and Program of Test

Experiments are conducted to study the effect of clear water scouring around slender structure embedded in sand bed of the channel section in laboratory flume. Piers are placed at the middle of the experimental channel section as shown in Figure 3.11.

A uniform sand bed of 5cm, 10cm and 15cm thick is prepared along the length of the channel from 4.8 m to 7.3 m. The sand is slightly compacted and leveled before starting the experiments. Initially the water is kept standing on the bed for few minutes then it is opened slowly to prevent the sand bed from excessive erosions. The depth of flow at different section of channel can be viewed from outside of the channel section by the scale attached on the side wall of the perspex sheet. The variation in the depth of scouring along the channel and in the vicinity of the pier can be directly observed through the scale attached at different sections at the pier face.

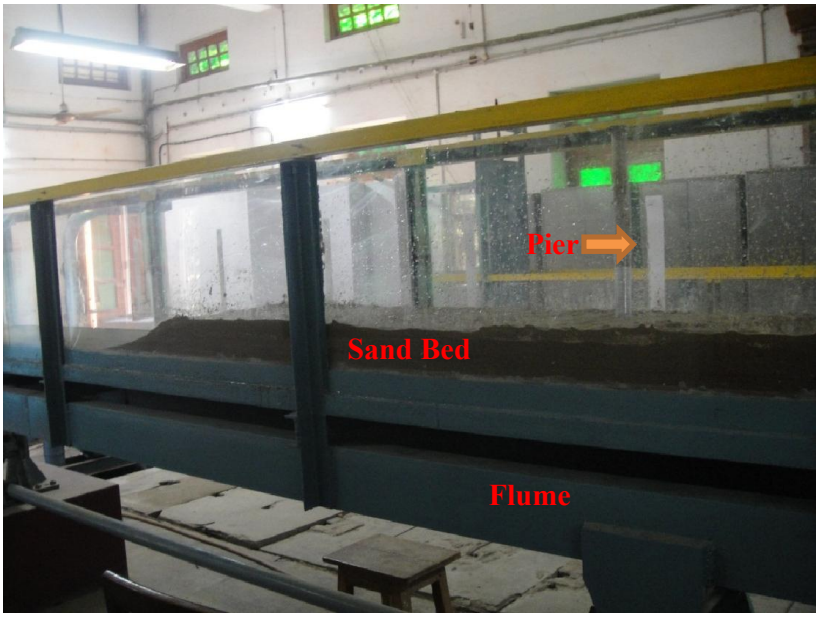

Figure 3.11: Piers embedded in sand bed

Steps involved in each experiment are as follows

- Preparation of sand bed and fixing of piers in the middle of the channel.
- Fixing of point gauge and ADV meter on the sliding platform.
- The discharge is controlled in the channel section and corresponding initial depth of water was measured above the sand bed.
- The rise in mercury column in the Venturi meter was measured at each flow and from the calibration curves actual discharge was calculated.
- The point velocity is measured by ADV meter.
- The depth of water at the upstream face of pier was measured in the pier through the attached scale on it (y).
- Position of Pier was taken as the origin (0) and scour depth reading was taken at 5 cm and 10cm of upstream and downstream respectively.

- Discharge was increased and the process was repeated for each piers. Many sets of reading were taken with the varying discharge and varying bed depth for each of model.
- The velocity profile and water surface elevation, scour depth at regular time intervals are measured at each experiment.
- The shape of scour hole is measured at the end of experiments by emptying the channel.

For each test, the primary measurements were flow velocity, water depth, and scour depth with time. Water depth and flow velocity were measured in the middle of the channel at 0.5 m upstream and downstream from the model. The depth average velocity was calculated from the measured vertical velocity profile and was used as one of the major parameters in the data analysis. The flow velocity was kept constant throughout the experiment. At the end, after emptying the channel, measurements of scour depth increment was carried out by the point gauge moving around the pier to find the location of maximum scour.

3.5 Experimental study on scouring around slender structure

The flow in a natural stream changes the dynamic boundary conditions continuously which lead to the changes in the scour pattern around hydraulic structure. The flow pattern around cylindrical, rectangular and oval obstruction that simulated as bridge pier is studied in the laboratory and the equilibrium scour depth is measured in the present study. The experiment in the channel has a full control on all the parameters, resulting in the data which may not be calculated in the field. Many observations are made; few of them are presented herein.

3.5.1 Scouring of sand bed around slender structure

Experiments are carried out to get an understanding on the scouring phenomenon around slender structure and consequent effect on channel morphology. Cylindrical, rectangular and oval shape model are placed in the middle of the channel and the scour depth is measured with time for varying discharge.

3.5.1.1 Scour depth variation around cylindrical shape pier

The flow characteristics around cylindrical piers models are studied extensively in Laboratory. The pier models are vertically mounted on the sand bed. The chances of erosion of sand bed is more for higher discharge in the flume, for that reason the thickness of sand bed were changed for each experiments. For lower discharge the thickness of bed was kept 5cm and for higher discharge it was 10 cm and 15 cm. The water flows around the pier by control manner in the flume. The discharge and depth of flow is monitored during experiment and measured.

The scour depth variations were measured around cylindrical piers of diameter 2.25cm with time for different discharge 150 liter/ minute to 350 liter/ minute. The scour depth (D_{sc}) at any time t is measured precisely by point gauge and the scale attached to the pier. The variation of non-dimensional scour depth (D_{sc}/d) is presented in Figure 3.12 with time.

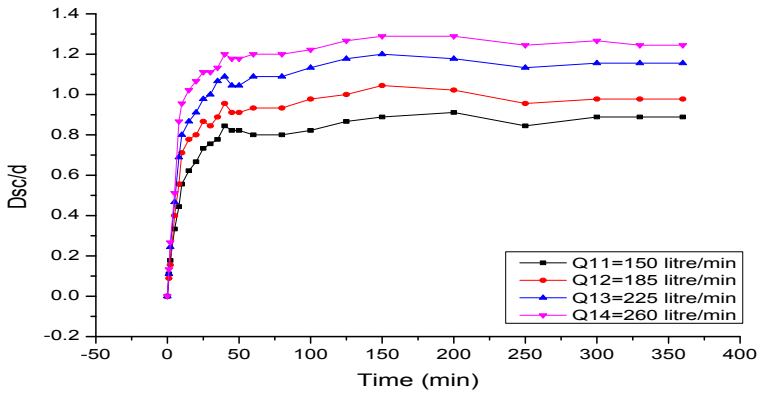

(a) Scour depth variation for cylindrical pier (d= 2.25 cm); sand depth (5 cm)

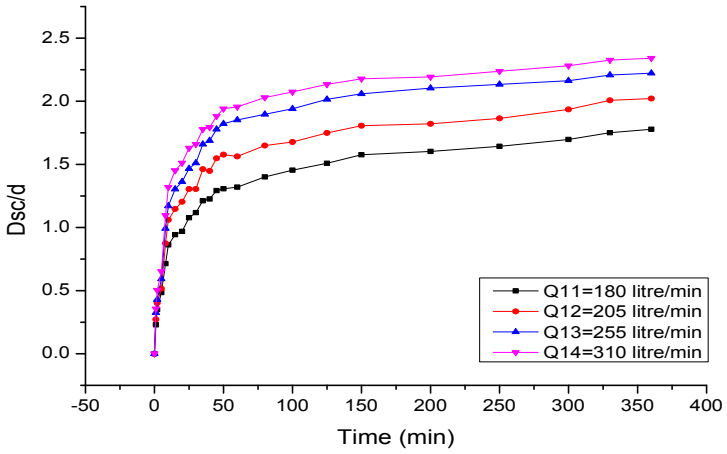

(b) Scour depth variation for cylindrical pier (d= 2.25 cm); sand depth (10 cm)

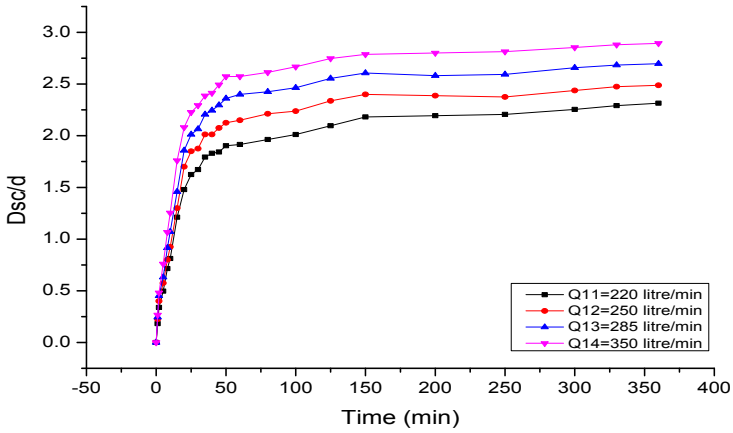

(c) Scour depth variation for cylindrical pier (d=2.25 cm); sand depth (15 cm)

Figure 3.12: Scour depth variation for cylindrical pier (d= 2.25 cm) of different discharges with time

It is observed from Figure 3.12 that on increasing the discharge the scour depth increases around piers. At initial stage, the rate of scouring is more around the pier and after sometimes the rate decreases. For a lower value of discharge, the scour hole grows slowly and attains the equilibrium state, after which the scour depth varies very slowly.

For the same pier, if increase the discharge the scour depth varies as shown in Figure 3.12 (a, b, c) respectively. Initially the scour depth increases and after few times the rate decreases and it is observed that after 300 minutes the rate is very less. The scour depth at different discharge shows the similar nature of scouring; only the amount of scouring increases with the discharge.

The experiments are carried out for different diameter of cylindrical piers for different discharges. To observe the effect of pier diameter in flow pattern and scouring hole formation around cylindrical pier of diameter 3.18cm, 3.86cm and 4.38cm, many experiments are conducted and results are presented in the following section.

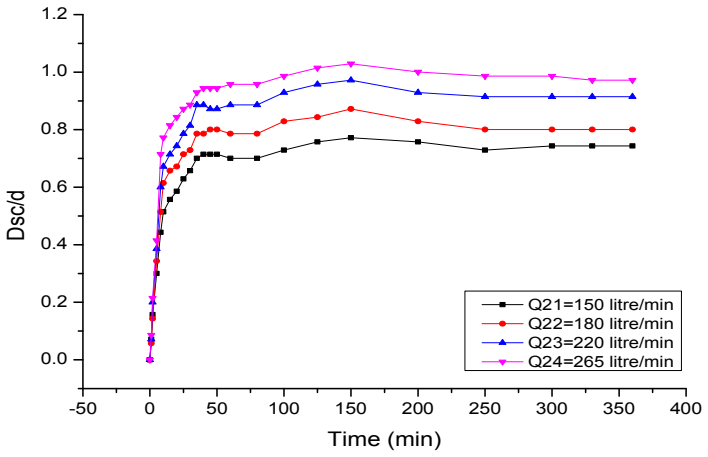

(a) Scour depth variation for cylindrical pier (d= 3.18 cm); sand depth (5 cm)

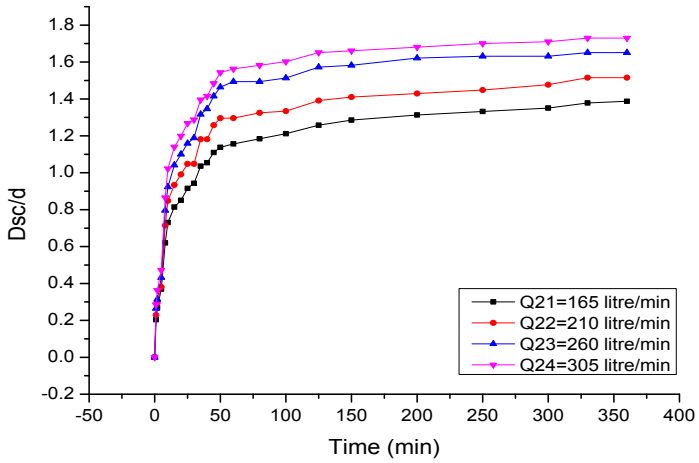

(b) Scour depth variation for cylindrical pier (d= 3.18 cm); sand depth (10 cm)

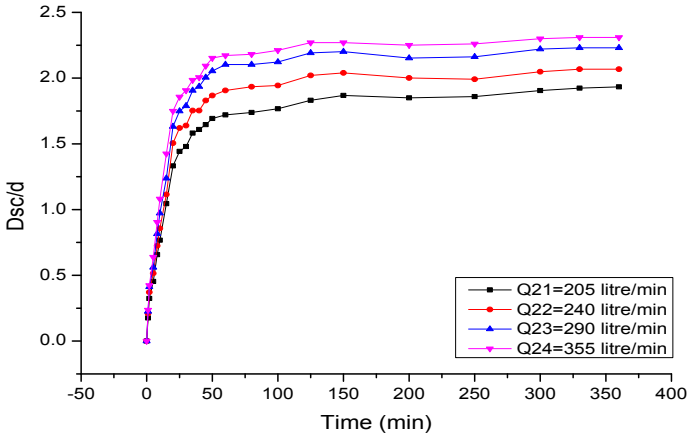

(c) Scour depth variation for cylindrical pier (d= 3.18 cm); sand depth (15 cm)

Figure 3.13: Scour depth variation for cylindrical pier (d= 3.18 cm) of different discharges with time

Scour depth variation with time is presented in figure 3.13 for pier 2 of diameter 3.18 cm at varying discharge from 150 to 355 lit/min. It is observed that, in case of 5 cm thick sand bed, the scour depth changes abruptly for discharge 180 lit/min and 220 lit/min after

50 minutes of the starting of experiments. After that it attains near about final stagnation point about 280 min.

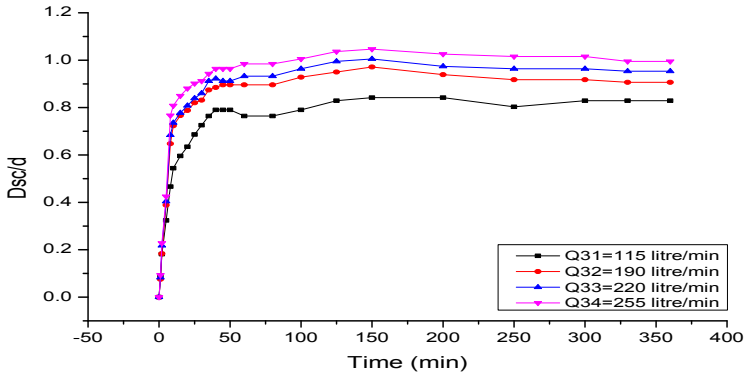

(a) Scour depth variation for cylindrical pier (d=3.86 cm); sand depth (5 cm)

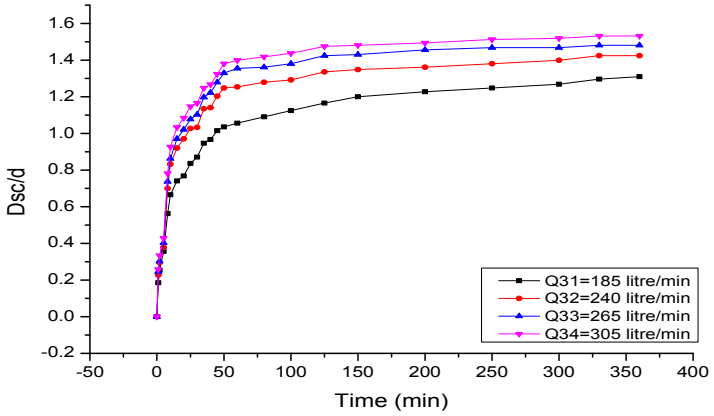

(b) Scour depth variation for cylindrical pier (d= 3.86 cm); sand depth (10 cm)

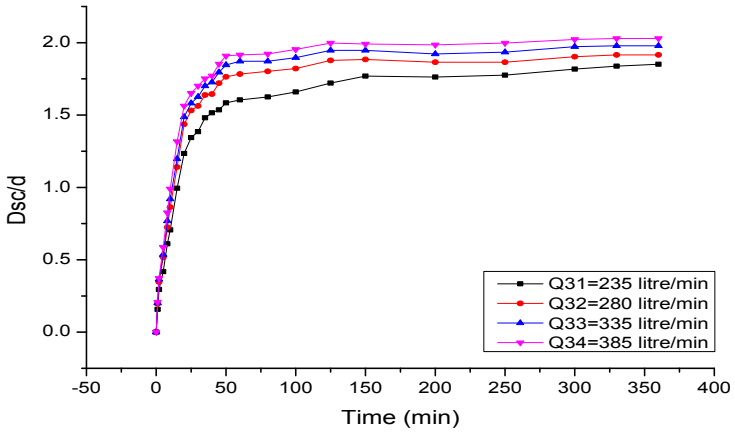

(c) Scour depth variation for cylindrical pier (d=3.86 cm); sand depth (15 cm)

Figure 3.14: Scour depth variation for cylindrical pier (d= 3.86 cm) of different discharges with time

The scour depth at any time is measured around pier of diameter 3.86cm and presented in Figure 3.14. It is observed from Figure 3.14 that scour depth increases linearly except 5 cm depth of sand for time less than 250 minute and the time to reach equilibrium scour depth is higher for 235 liter/minute, the equilibrium scour depth reached in shorter time.

The maximum sour depth around the pier of diameter 4.38cm is measured and presented in Figure 3.15. The discharge is varied from 145 liter/minute to 360 liter/minute and it is observed that the rate of change of increasing the scour depth is take longer time than less diameter piers. Increase in pier diameter, flow pattern changes and horseshoe vortex formation observed. With the increase in discharge for large pier diameter the scour-depth vary exponentially.

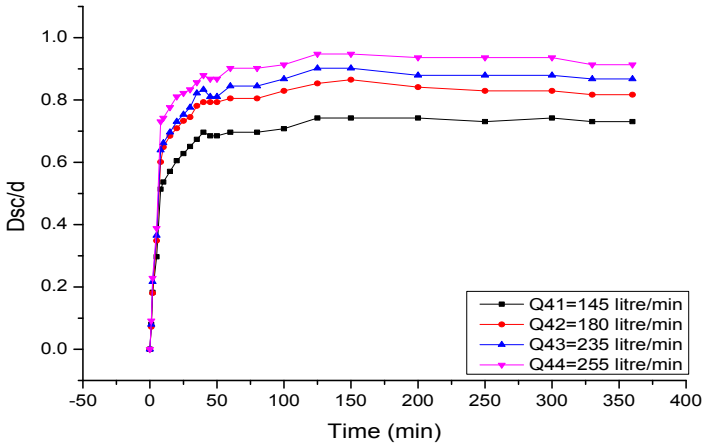

(a) Scour depth variation for cylindrical pier (d= 4.38 cm); sand depth (5 cm)

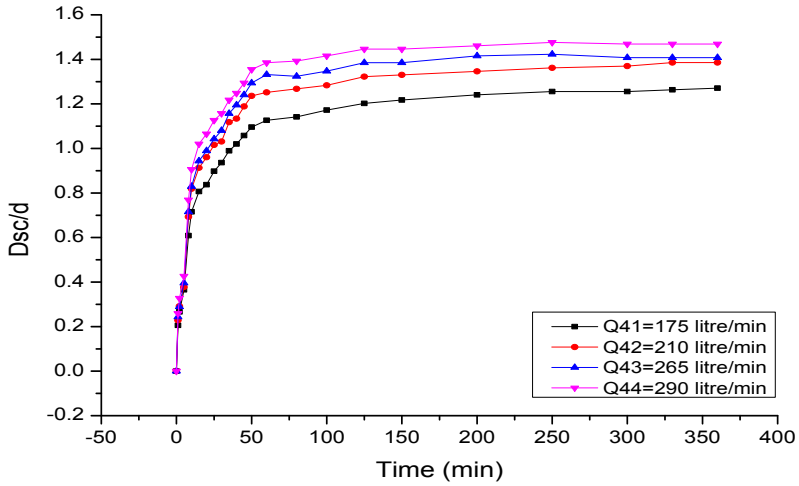

(b) Scour depth variation for cylindrical pier (d= 4.38 cm); sand depth (10 cm)

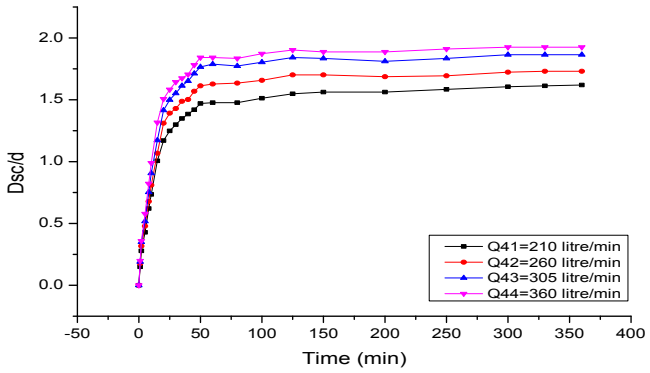

(c) Scour depth variation for cylindrical pier (d= 4.38 cm); sand depth (15 cm)

Figure 3.15: Scour depth variation for cylindrical pier (d= 4.38 cm) of different discharges with time

3.5.1.2 Scour depth variation around rectangular shape pier

The scour depth around rectangular shape pier of dimensions 3.38 cm x 3.04 cm and 4.15 cm x 4.04 cm are measured for different discharges. The variation of scour depth variation around rectangular pier with time is presented in Figure 3.16 and Figure 3.17 respectively. The discharge is varied from 140 liter/ minute to 350 liter/ minute and scour depth variation is observed in regular interval.

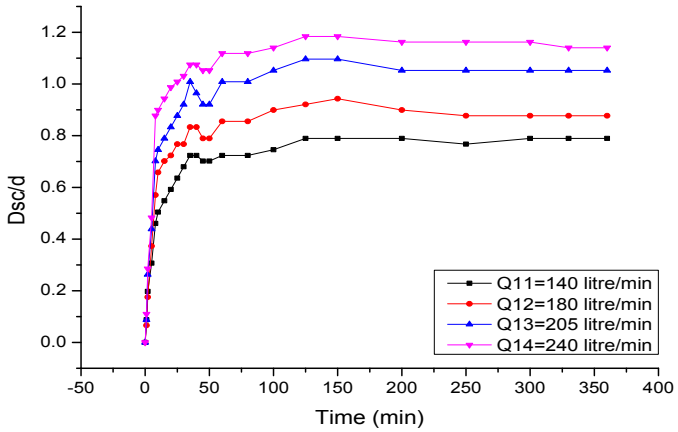

(a) Scour depth variation for rectangular pier (3.38 X 3.04 cm); sand depth (5 cm)

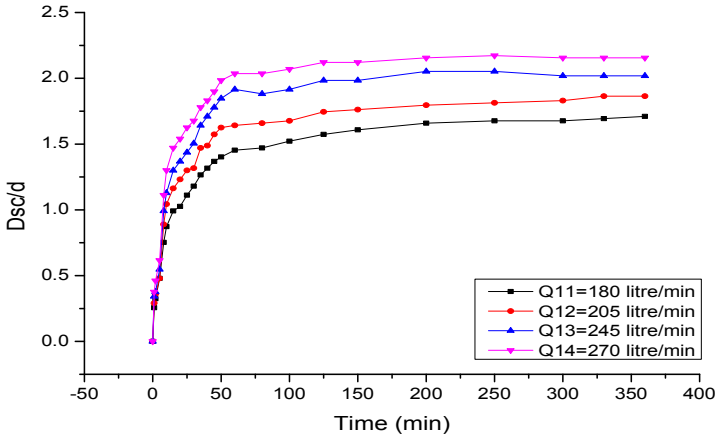

(b) Scour depth variation for rectangular pier (3.38 X 3.04 cm); sand depth (10 cm)

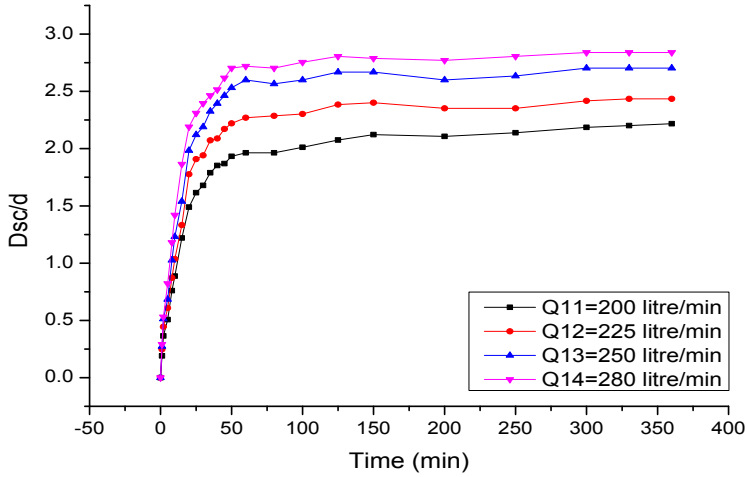

(c) Scour depth variation for rectangular pier (3.38 X 3.04 cm); sand depth (15 cm)

Figure 3.16: Scour depth variation for Rectangular pier (R1 = 3.38 X 3.04 cm) for different discharges with time

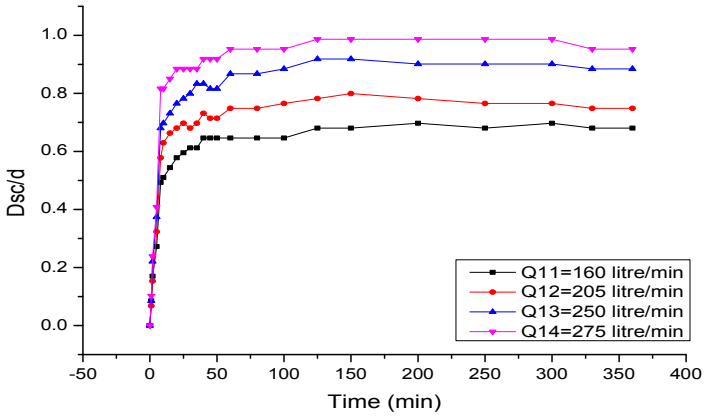

(a) Scour depth variation for rectangular pier (4.15 X 4.04 cm); sand depth (5 cm)

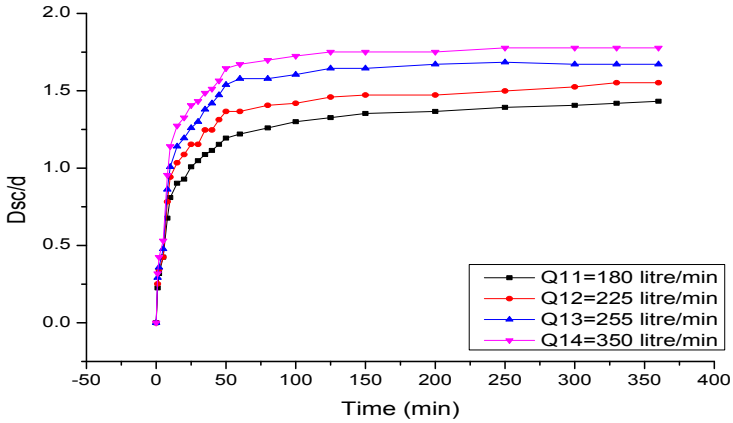

(b) Scour depth variation for rectangular pier (4.15 X 4.04 cm); sand depth (10 cm)

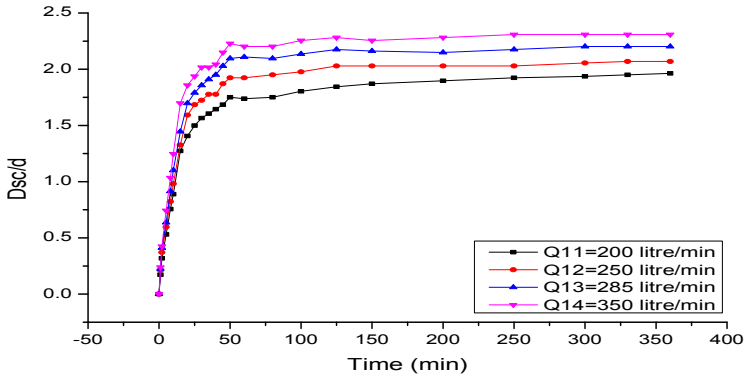

(c) Scour depth variation for rectangular pier (4.15 X 4.04 cm); sand depth (15 cm)

Figure 3.17: Scour depth variation for Rectangular pier (R2 = 4.38 X 4.04 mm) of different discharges with time

3.5.1.3 Scour depth variation around oval shape pier

The scour depth around oval shape pier is measured with time for different discharge in the channel section. The maximum and minimum characteristic length of oval shape pier in plan form is 2.9cm x 1.5cm and 4.7cm x 3cm respectively. The shorter dimensions are placed to obstruct the flow path. The development of scour hole around these structures is measured with time. The scour depths around these piers are presented in Figure 18 and Figure 19. The rate of scouring initially was high and the scouring occurs for long time and the rate was very slow.

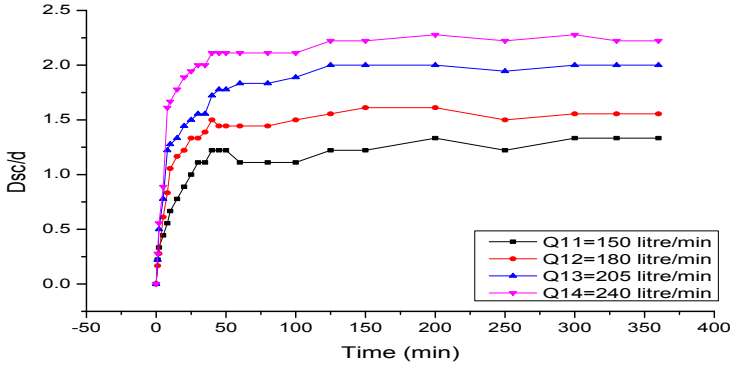

(a) Scour depth variation for oval pier (2.9 X 1.5 cm); sand depth (5 cm)

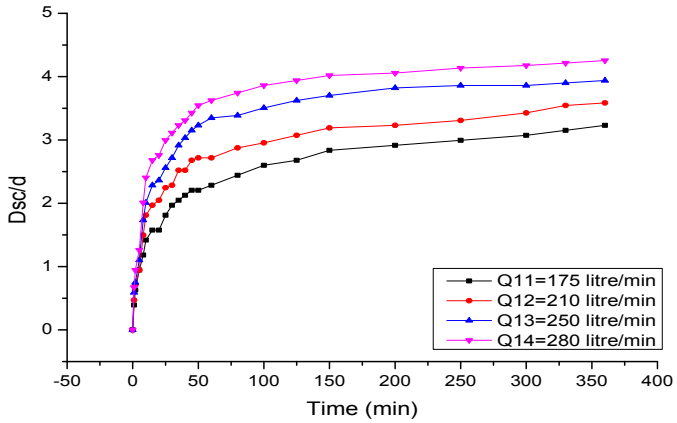

(b) Scour depth variation for oval pier (2.9 X 1.5 cm); sand depth (5 cm)

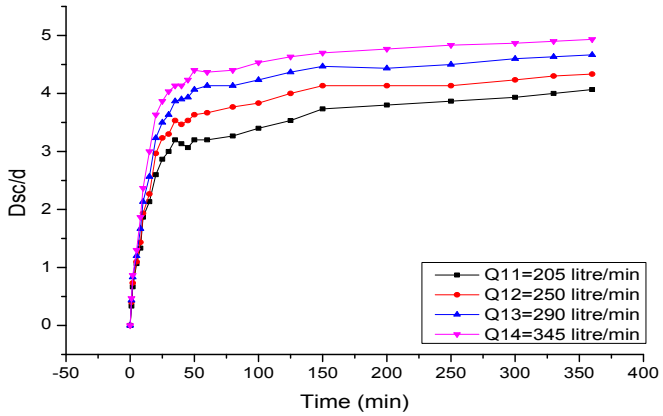

(c) Scour depth variation for oval pier (2.9 X 1.5 cm); sand depth (15 cm)

Figure 3.18: Scour depth variation for Oval pier (O1 = 2.9 X 1.5 cm) of different discharges with time

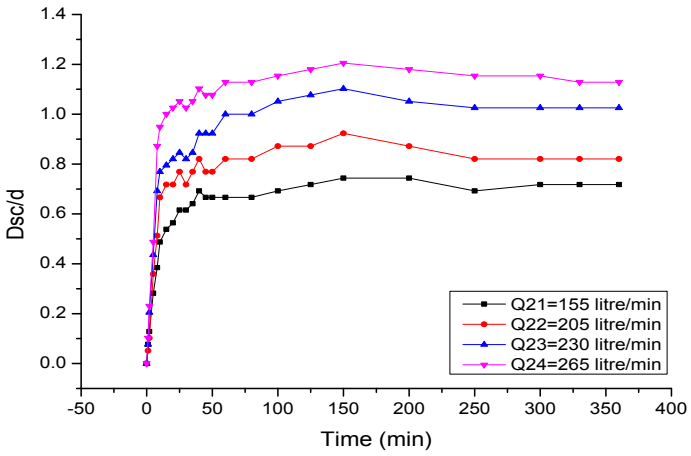

(a) Scour depth variation for oval pier (4.7 X 3 cm); sand depth (5 cm)

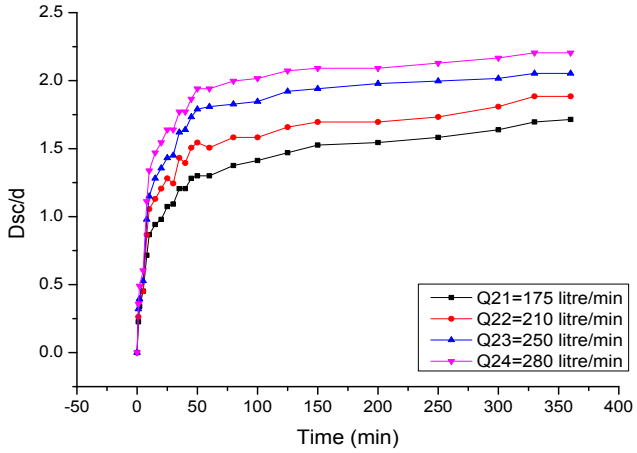

(b) Scour depth variation for oval pier (4.7 X 3 cm); sand depth (10 cm)

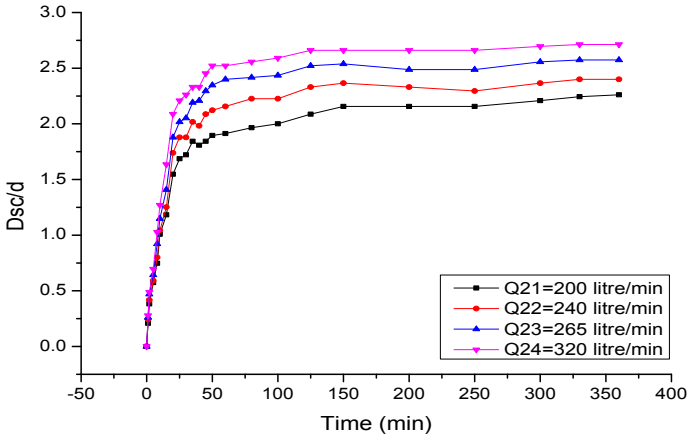

(c) Scour depth variation for oval pier (4.7 X 3 cm); sand depth (15 cm)

Figure 3.19: Scour depth variation for oval pier (O2 = 4.7 X 3 cm) for different discharges with time

3.5.2 Effect of shape and size of slender structure on scour depth

The scour rate for the flume tests on the cylindrical, rectangular and oval shape slender structures having the same dimensions are compared for different discharge. The rate of scour depth around these structures is presented in Figure 3.20 to 3.22. The shorter dimension is kept transverse to the flow direction. The shape of a bridge pier can strongly affect the flow pattern around the flow pattern around it. In this study, cylindrical, rectangular and oval piers are considered. Bridge piers are most often installed with the longer side parallel to the major flow direction. Therefore the length over width ratio (L/B) is kept greater than one for all piers in the study.

The diameter of cylindrical piers was 3.18cm and the shorter size of the rectangular pier was 3.04cm. The characteristics diameter of both piers is approximately equal. The diameter of cylindrical piers is kept 3.18cm and the shorter size of the rectangular pier is kept 3.04 cm. The characteristics diameter of both piers is approximately equal.

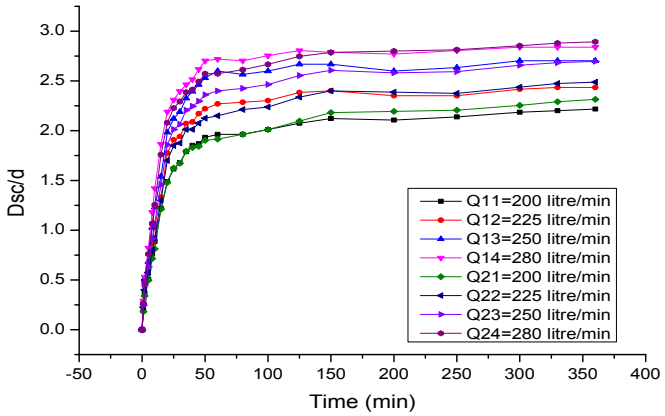

Figure 3.20: Comparison of scour depth between Cylindrical (diameter 3.18 cm) and Rectangular (3.38 X 3.04 cm) pier with different discharges with time

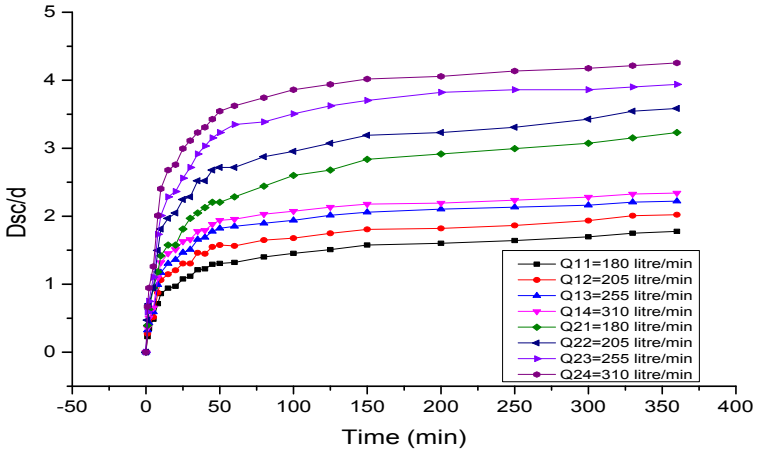

Figure 3.21: Comparison of scour depth between Cylindrical (diameter 2.25 cm) and Oval (2.9 X 1.5 cm) pier for different discharges with time

The rate of scouring is measured for oval of characteristic length 3cm and shorter dimension of rectangle for different discharge.

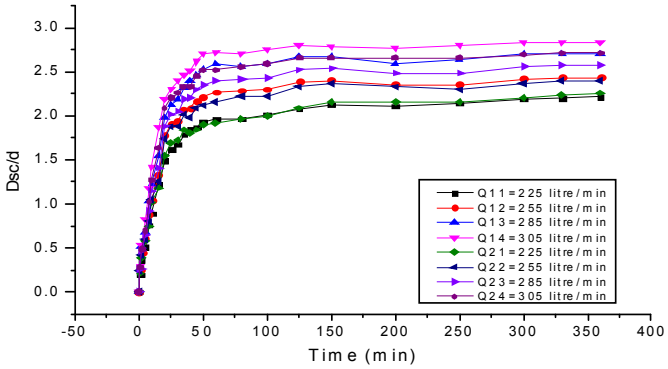

Figure 3.22: Comparison of scour depth between Rectangular (3.38 X 3.04 cm) and Oval (4.7 X 3 cm) for different discharges with time

In case of rectangular shape pier, the rate of scouring is more compared to cylindrical and oval shape pier. The horse shoe vortex is formed for low discharge to high discharge.

The scour depth around different size of piers for different discharge is presented in the Figure 3.23 (a) –(c). The depth of sand was increased for increasing value of discharge and depth of flow.

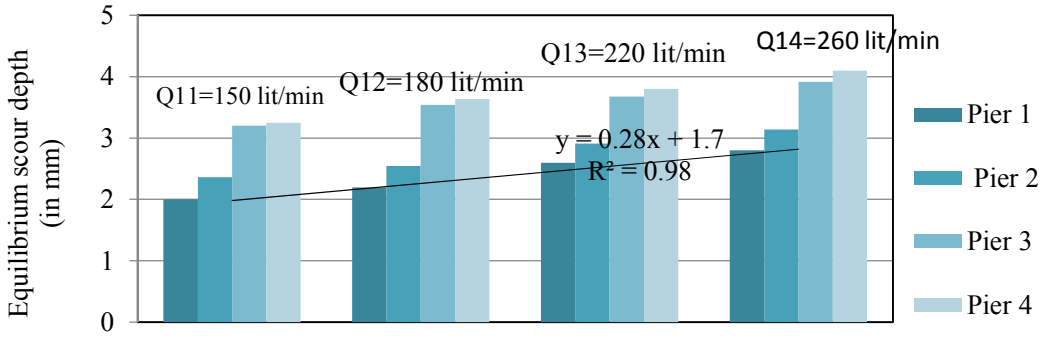

(a)

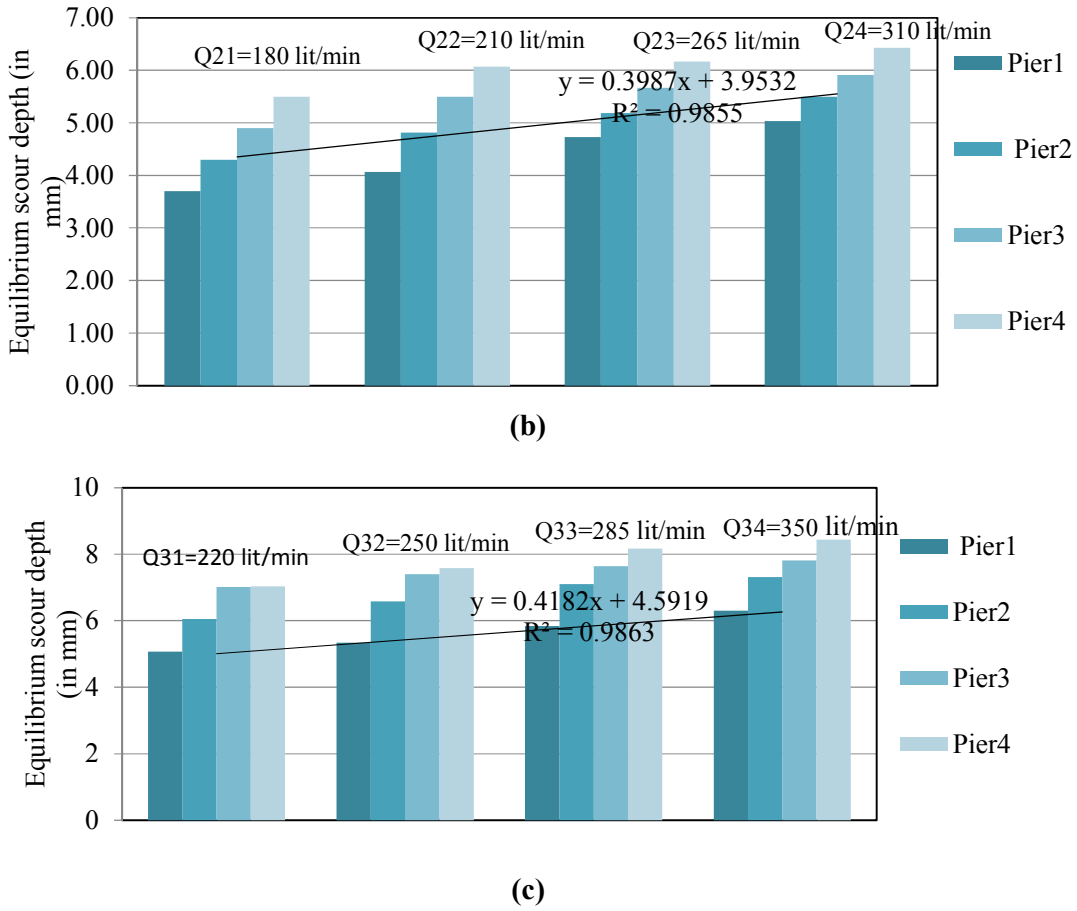

Figure 3.23: Equilibrium scour depth around cylindrical pier with different discharges

Analysis shows that the equilibrium scour depth is always less for smaller size pier in comparison of larger size pier. This equilibrium scour depth follows almost same pattern for piers at different values of discharge. The equilibrium scour depth is increase with increase in discharges.

All the piers were installed with a 0-degree attack angle in the middle of the flume. Major scour always occurred around the corner of the rectangular pier but only maximum scour depth was used in the analysis. The shapes of the scour holes for different pier were recorded and compared. In addition cylindrical pier with a diameter equal to the width of rectangular pier were used as the reference case. The results indicate that there are noticeable effects on scour depth, due to pier shape. As can be seen, the rectangular piers

consistently have large initial scour rates than the cylindrical and oval pier. Therefore it is concluded that around rectangular pier maximum scour depth occur.

3.5.2.1 Contour of scour hole and schematic representation of development of scouring

The shape and form of channel bed is investigated for cylindrical, rectangle and oval shape piers after receding water from flume. Initial sand depth of bed was 10 cm and discharge passes 230 liter/ minutes for all three cases. The formation of scour hole is observed around piers and measurement of scour depth was done with respect to original bed level. The contour of the hole around the piers is schematically presented in Figure 3.24 to 3.26.

Depending on the approaching flow conditions and scour hole shape, the topography of scour holes are as follows.

The scour hole at cylindrical pier develops through the sand-layer in the upstream mainly. The scour hole does not extend beyond the downstream edge of the pier. The sand-layer remains intact in the downstream of the pier and around the upstream perimeter of the scour hole [Figure 3.24].

The scour hole at rectangular pier forms through the sand-layer in the upstream and downstream. The sand-layer remains intact in the downstream of the scour hole and around the upstream perimeter of the scour hole [Figure 3.25].

The sand-layer disintegrates over a long distance downstream but remains intact around the upstream perimeter of the scour hole around oval pier. [Figure 3.26]

The relative size of the scour hole produced by the rectangular pier was observed to be much larger than in other cases. Also, in case of the rectangular pier, the scour hole surrounds the entire pier.

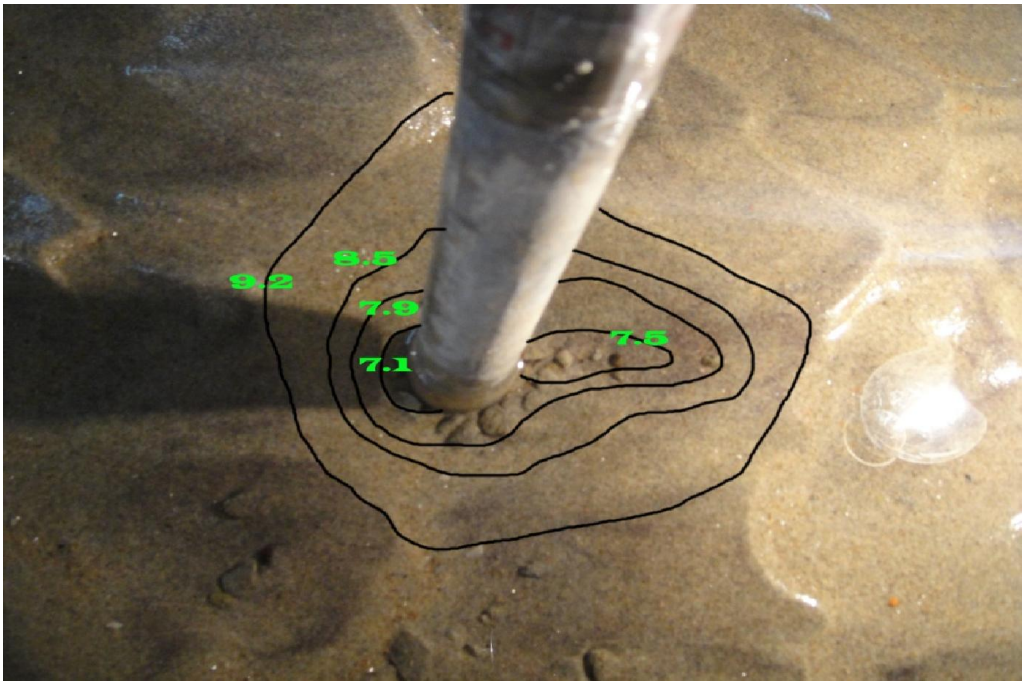

(a)

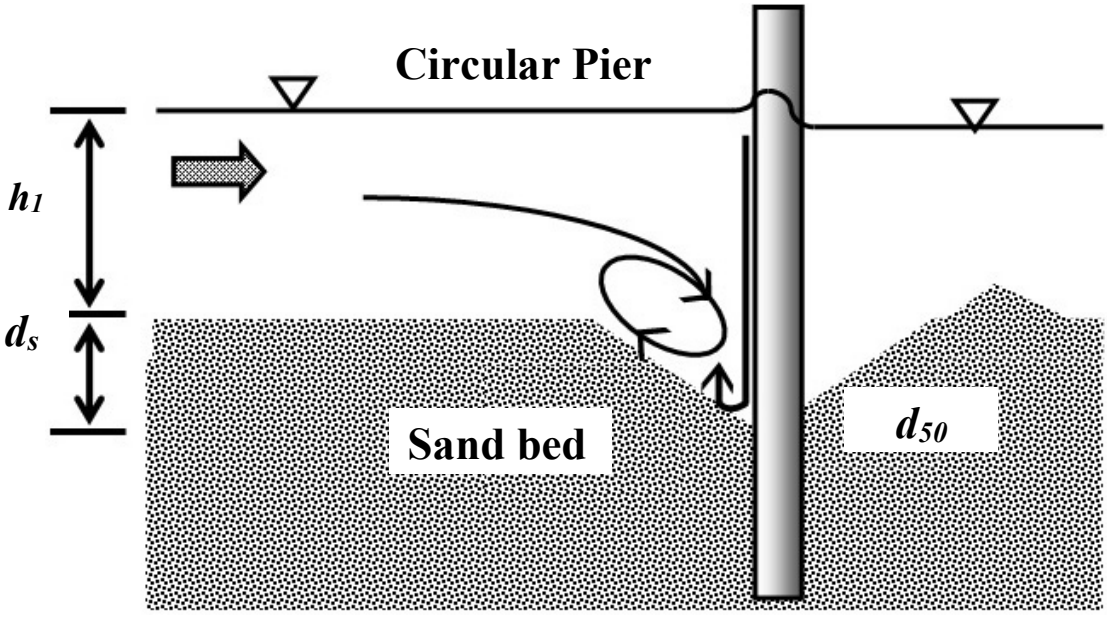

Figure 3.24 (a): Contour of cylindrical pier for scouring, (b): Scouring sketch diagram of Contour for cylindrical pier

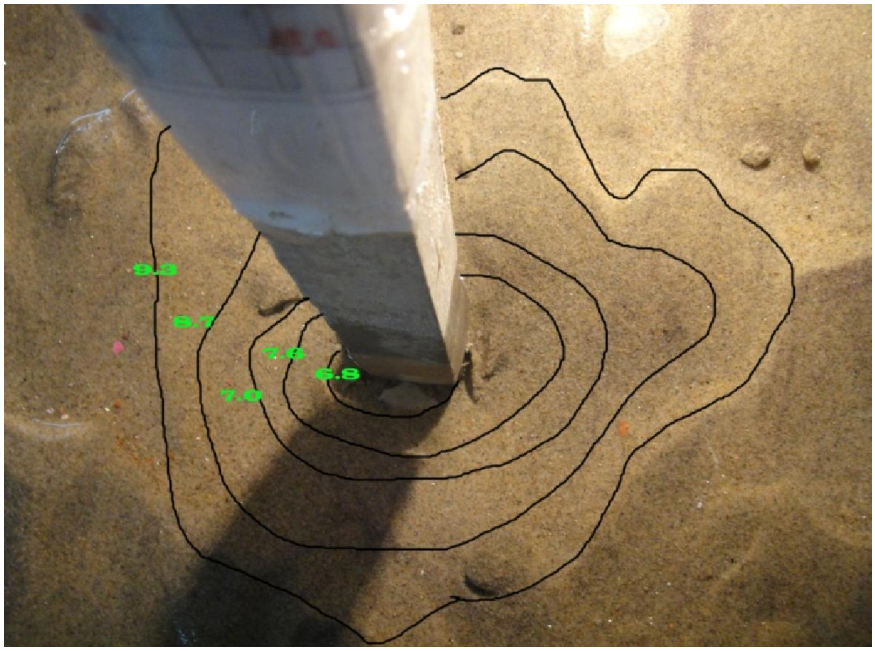

(a)

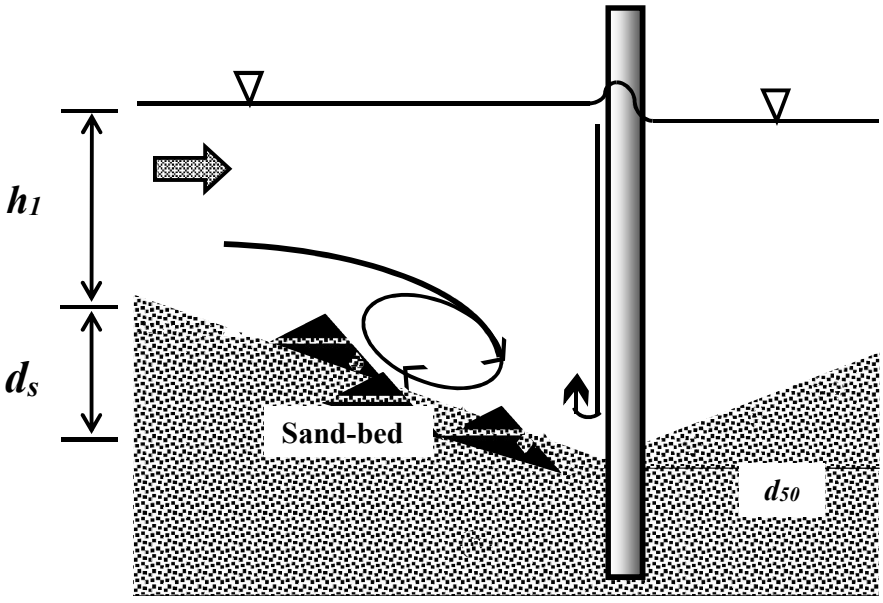

Figure 3.25 (a): Contour of rectangular pier for scouring, (b): Scouring sketch diagram of Contour for rectangular pier

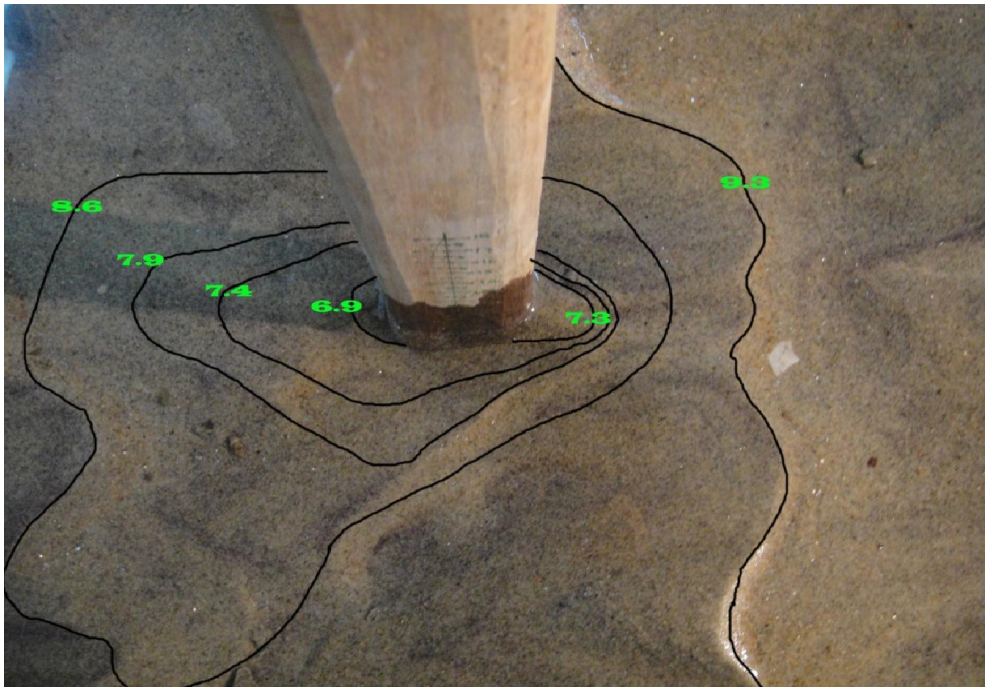

(a)

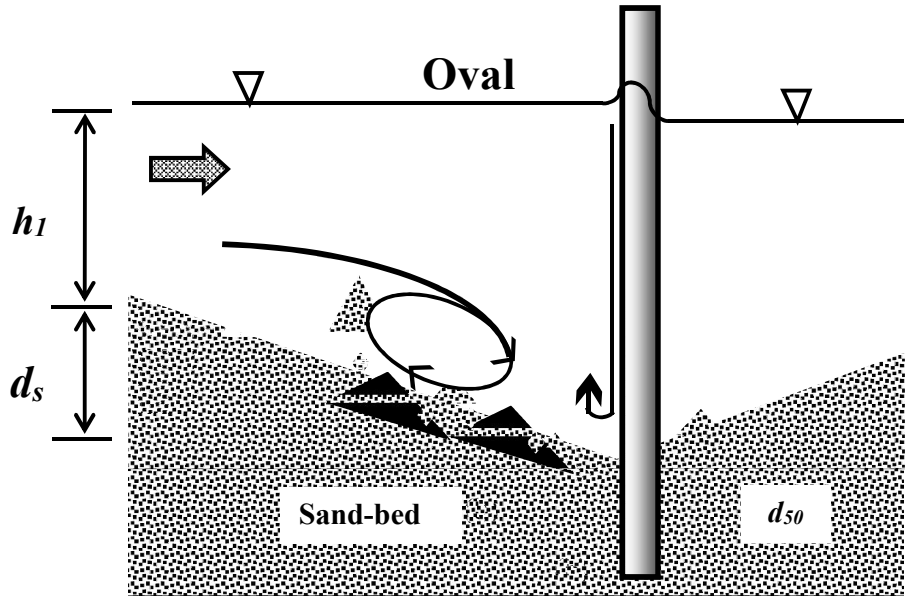

Figure 3.26 (a): Contour of Oval pier for scouring, (b): Scouring sketch diagram of Contour for oval pier

3.5.3 Parametric study of Non-dimensional Scour depth around slender structure

The maximum scour depths around different piers after completion of each experiment are measured. The data obtained in the experiment is analyzed for scouring around slender structure.

Experimental analysis results for cylindrical pier are presented herein in the Table 3.1 to 3.4. The cylindrical piers of diameter 2.25cm, 3.18cm, 3.86 cm and 4.38cm are denoted by pier1, pier2, pier3 and pier4 respectively. The channel width b, pier diameter d and depth of flow y.

Table 3.1: Analysis data for Pier 1

Discharge (Q) lit/min	Flow Depth y (in cm)	Avg. Vel. (Vav) (m/s)	Equi. Scour Depth (dse) (cm)	y/d	dse/d	Q/b
150	1.7	0.367	2	0.0756	0.889	0.375
185	1.95	0.395	2.2	0.0867	0.978	0.4625
225	2.1	0.446	2.6	0.0933	1.156	0.5625
260	2.3	0.471	2.8	0.1022	1.244	0.65

Table 3.2: Analysis data for Pier 2

Discharge (Q) lit/min	Flow Depth y (in cm)	Avg. Vel. (Vav) (m/s)	Equi. Scour Depth (dse) (cm)	y/d	dse/d	Q/b
150	1.5	0.417	2.36	0.0472	0.743	0.375
180	1.6	0.469	2.55	0.0503	0.800	0.45
220	1.8	0.509	2.91	0.0566	0.915	0.55
265	1.9	0.581	3.14	0.0597	0.986	0.6625

Table 3.3: Analysis data for Pier 3

Discharge (Q) lit/min	Flow Depth y (in cm)	Avg. Vel. (Vav) (m/s)	Equi. Scour Depth (dse) (cm)	y/d	dse/d	Q/b
155	1.7	0.380	3.2	0.0440	0.829	0.3875
190	1.9	0.417	3.54	0.0492	0.918	0.475
220	2	0.458	3.68	0.0518	0.953	0.55
255	2.1	0.506	3.92	0.0544	1.016	0.6375

Table 3.4: Analysis data for Pier 4

Discharge (Q) lit/min	Flow Depth y (in cm)	Avg. Vel. (Vav) (m/s)	Equi. Scour Depth (dse) (cm)	y/d	dse/d	Q/b
145	1.6	0.378	3.25	0.0365	0.742	0.3625
180	1.8	0.417	3.63	0.0411	0.829	0.45
235	2.1	0.466	3.8	0.0479	0.868	0.5875
255	2.2	0.483	4.1	0.0502	0.936	0.6375

Table 3.5: Analysis data for Pier 5

Discharge (Q) lit/min	Flow Depth y (in cm)	Avg. Vel. (Vav) (m/s)	Equi. Scour Depth (dse) (cm)	y/d	dse/d	Q/b
140	1.8	0.324	2.40	0.0533	0.710	0.35
180	1.95	0.385	2.67	0.0577	0.789	0.45
205	2.2	0.388	3.20	0.0651	0.947	0.5125
240	2.3	0.435	3.53	0.0680	1.045	0.6

Table 3.6: Analysis data for Pier 6

Discharge (Q) lit/min	Flow Depth y (in cm)	Avg. Vel. (Vav) (m/s)	Equi. Scour Depth (dse) (cm)	y/d	dse/d	Q/b
160	1.6	0.417	2.67	0.0386	0.643	0.4
205	2	0.427	3.00	0.0482	0.723	0.5125
250	2.2	0.473	3.53	0.0530	0.851	0.625
275	2.3	0.498	3.87	0.0554	0.932	0.6875

Table 3.7: Analysis data for Pier 7

Discharge (Q) lit/min	Flow Depth y (in cm)	Avg. Vel. (Vav) (m/s)	Equi. Scour Depth (dse) (cm)	y/d	dse/d	Q/b
150	1.7	0.368	2.000	0.1133	1.333	0.375
180	2	0.375	2.333	0.1333	1.556	0.45
205	2.1	0.407	3.000	0.1400	2.000	0.5125
240	2.2	0.455	3.417	0.1467	2.278	0.6

Table 3.8: Analysis data for Pier 8

Discharge (Q) lit/min	Flow Depth y (in cm)	Avg. Vel. (Vav) (m/s)	Equi. Scour Depth (dse) (cm)	y/d	dse/d	Q/b
155	1.9	0.340	2.15	0.1267	1.436	0.3875
205	2	0.427	2.46	0.1333	1.641	0.5125
230	2.1	0.456	3.08	0.1400	2.051	0.575
265	2.3	0.480	3.54	0.1533	2.359	0.6625

3.5.3.1 Variation of Non-dimensional Scour depth around piers model

The maximum scour depth around cylindrical, rectangular and oval model pier is measured for different flow velocity and depth of flow. The approach velocity is measured by ADV meter near the piers. The variation of D_{se}/d with V_{av}/ V_{app} is presented in the Figures 3.27 to 3.29.

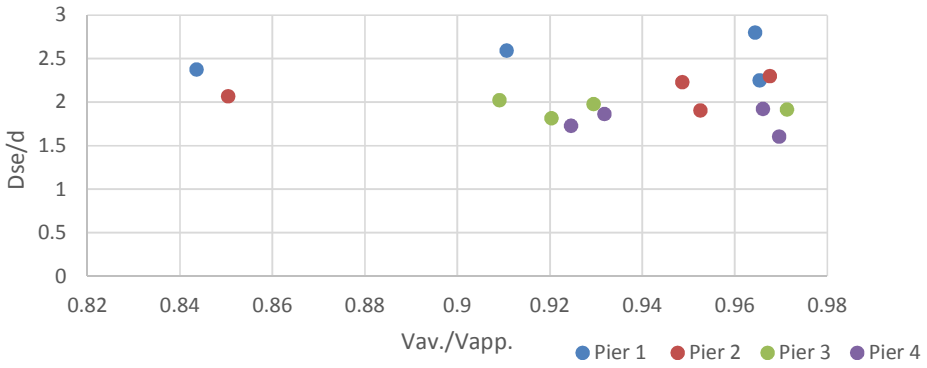

Figure 3.27: Variation of (Dse/d) vs (Vav./Vapp.) of Cylindrical Piers with different discharges

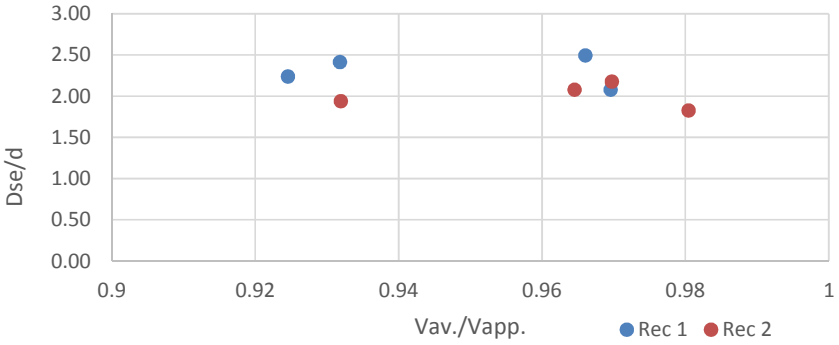

Figure 3.28: Variation of (Dse/d) vs (Vav./Vapp.) of Rectangular Piers (1 & 2) with different discharges

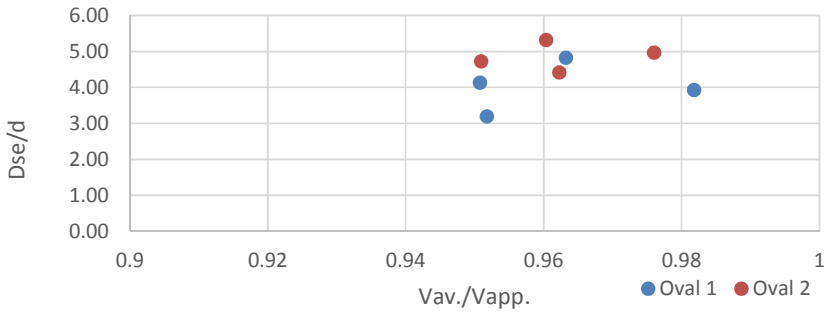

Figure 3.29: Variation of (Dse/d) with (Vav./Vapp.) of oval piers (1 & 2) for different discharges

The variation of (D_{se}/d) with y/b is observed and presented in Figure 3.30 to 3.33 for cylindrical, rectangular and oval shape pier.

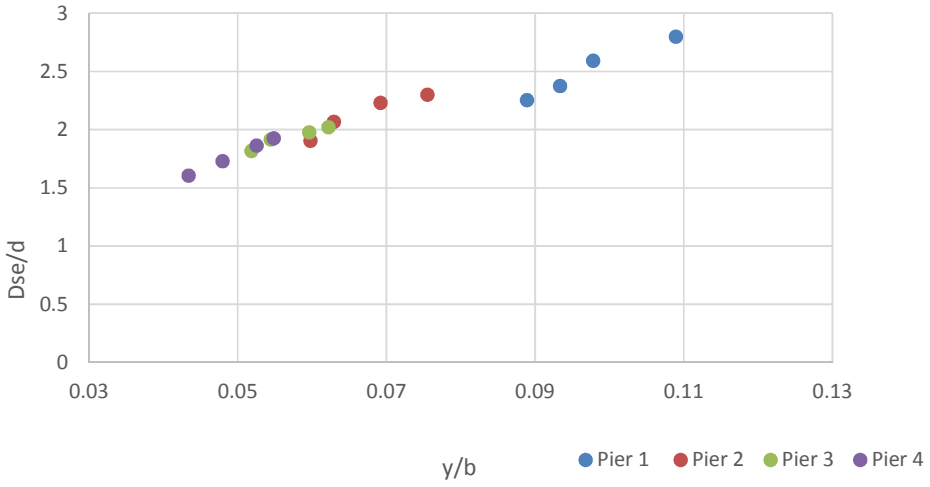

Figure 3.30: Variation of (Dse/d) with y/b of Cylindrical Piers with different discharges

The result shows that increase in flow depth with respect to channel width (y/b), dimensionless parameter (Dse/d) also increases.

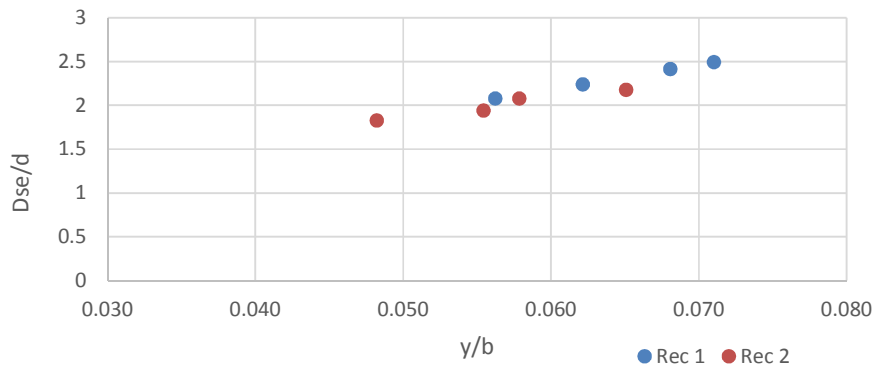

Figure 3.31: Variation of Dse/d with y/b of Rectangular Piers with different discharges

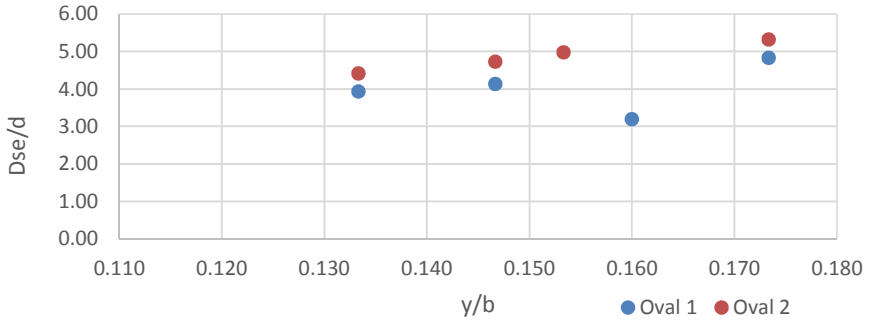

Figure 3.32: Variation of Dse/d with y/b of oval piers for different discharges

The variation of Dse/d with Q/b plotted in Figure 3.33 to 3.36 for cylindrical, rectangular and oval model.

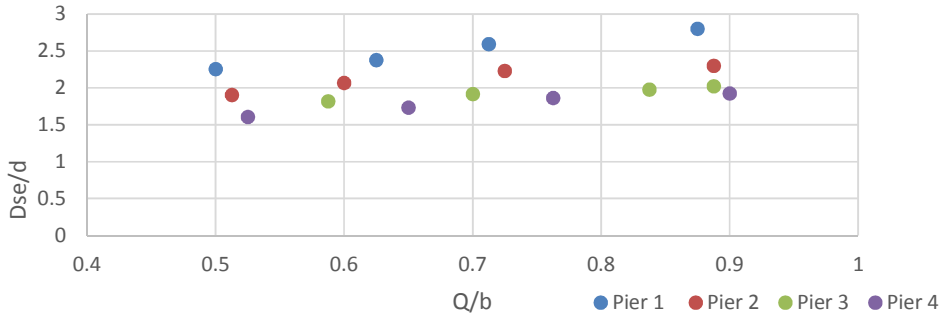

Figure 3.33: Variation of (Dse/d) with Q/b of Cylindrical Piers with different discharges

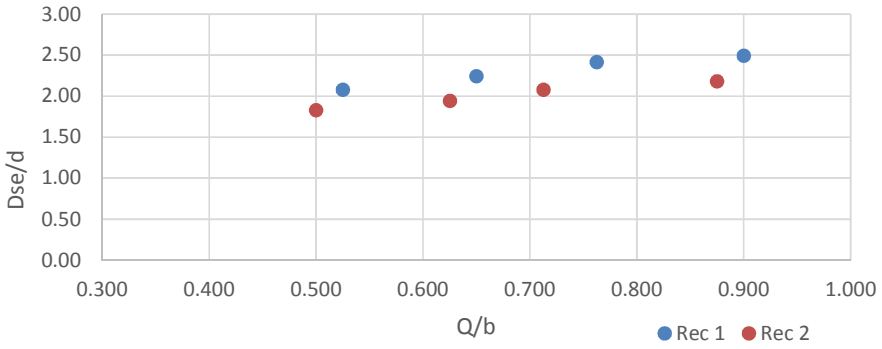

Figure 3.34: Variation of Dse/d with Q/b of Rectangular Piers (1 & 2) for different discharges

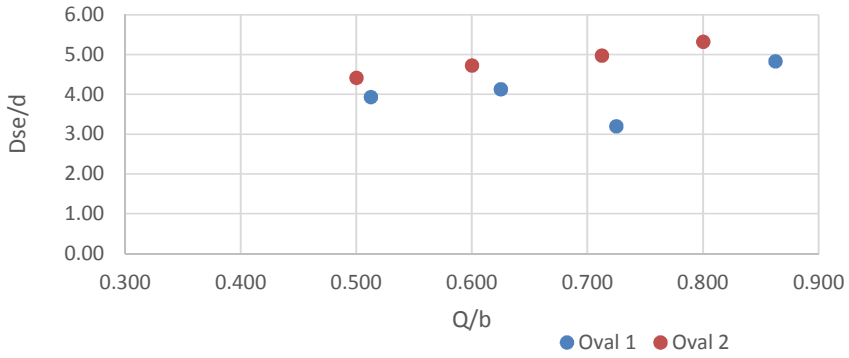

Figure 3.35: Variation of Dse/d with Q/b of oval piers (1 & 2) for different discharges

Proposed equation for prediction on equilibrium scour depth

Regression analysis is carried on to find the relationship between non-dimensional parameters D_{se} / d with y/b, V_{av}/ V_{app} and Q/b in the form of polynomial and exponential. The equilibrium scour depth may be predicted by following regression equations.

Predicted scour depth for cylindrical shape model

D_{se} / d = -1631.9 $(y/b)^2$ + 245.1 (y/b) – 6.905, R^2 = 0.9964

D_{se} / d = -840.09 $(V_{av}/ V_{app})^2$ + 1591.3 (V_{av}/ V_{app}) – 751.4, R^2 = 0.599

D_{se} / d = 0.8657 $e^{10.895(y/b)}$, R^2 = 0.9502

D_{se} / d = 1.01 ln(Q/b) + 2.91, R^2 = 0.965

Predicted scour depth for rectangular shape model

$D_{se}/d = -526.22 (V_{av}/V_{app})^2 + 1004.5 (V_{av}/V_{app}) - 477.19$, $R^2 = 0.7869$

$D_{se}/d = -0.818 (Q/b)^2 + 2.091 (Q/b) - 0.98$, $R^2 = 0.981$

$D_{se}/d = 1.08\ e^{10.76(y/b)}$, $R^2 = 0.945$

$D_{se}/d = 0.6163 \ln(y/b) + 2.005$, $R^2 = 0.9835$

Predicted scour depth for oval shape model

$D_{se}/d = -169.57 (y/b)^2 + 74.97 (y/b) - 2.57$, $R^2 = 0.991$

$D_{se}/d = -4339.88 (V_{av}/V_{app})^2 + 8397.2 (V_{av}/V_{app}) - 4057.1$, $R^2 = 0.571$

$D_{se}/d = 2.38\ e^{4.66(y/b)}$, $R^2 = 0.976$

$D_{se}/d = 1.84 \ln(Q/b) + 5.67$, $R^2 = 0.978$

3.5.4 Visualization of vortex motion around pier model

The scour hole at a pier forms beneath the horseshoe vortex, which sinks into the hole as scouring progresses. The hydrodynamic forces (namely drag and lift forces) acting on the sediment particles owing to the vortex flow remove the bed particles and decrease with an increase in scour depth. The sediment particles are mainly dislodged from this region by the action of the vortex and are carried downstream by the sides of the pier.

When the water flow in river is deflected by obstructions like piers scouring would occur arising from the formation of vortexes. Owing to the formation of this vertical vortex, sand bed material is continuously removed so that holes are formed at the sand bed and this result in local scour of bridge piers. As the shape of vortices looks like horseshoes, it is sometimes called horseshoe vortex.

For visualization of vortex motion around slender structure video is taken after 2 hour, when steady state condition is achieved within interval of 3-5 seconds with HD camera from outside the flume near perpex sheet. Here in figure 3.36 – 3.38, few snaps are present here.

(a) Visualization of vortex motion around cylindrical slender structure at time 0.01 sec

(b) Visualization of vortex motion around cylindrical slender structure at time 0.04 sec

(c) Visualization of vortex motion around cylindrical slender structure at time 0.07 sec

(d) Visualization of vortex motion around cylindrical slender structure at time 0.09 sec

Figure 3.36: Visualization of vortex motion around cylindrical slender structure

(a)Visualization of vortex motion around rectangular slender structure at time 0.01 sec

(b)Visualization of vortex motion around rectangular slender structure at time 0.04 sec

(c)Visualization of vortex motion around rectangular slender structure at time 0.06 sec

(d)Visualization of vortex motion around rectangular slender structure at time 0.10 sec

Figure 3.37: Visualization of vortex motion around rectangular slender structure

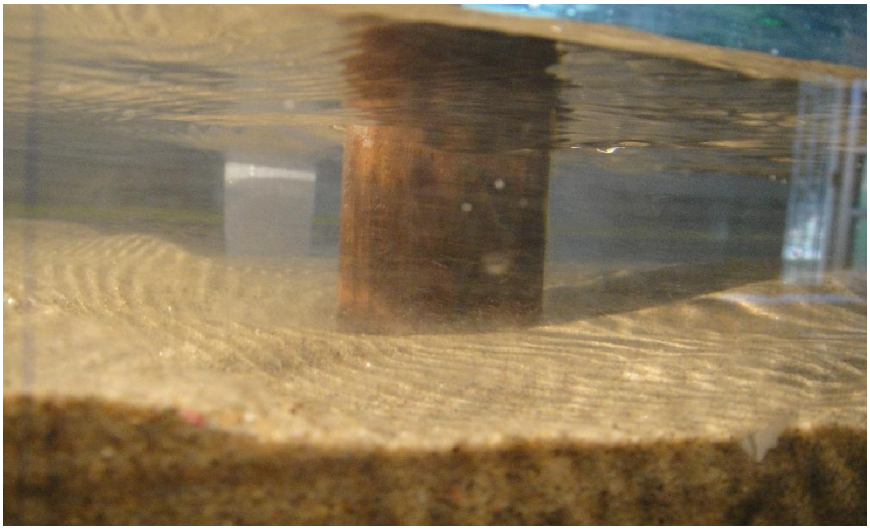

(a)Visualization of vortex motion around oval slender structure at time 0.01 sec

(b)Visualization of vortex motion around oval slender structure at time 0.04 sec

(c)Visualization of vortex motion around oval slender structure at time 0.08 sec

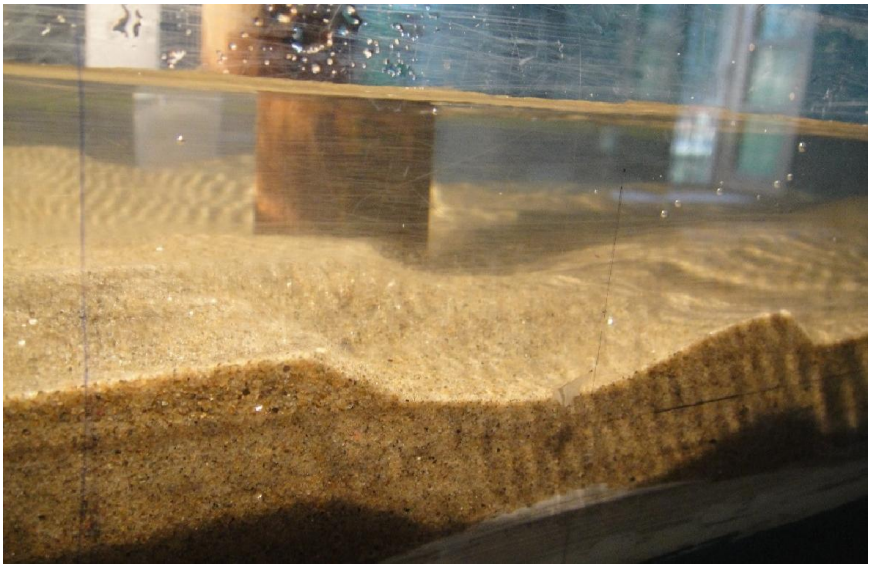

(d)Visualization of vortex motion around oval slender structure at time 0.10 sec

Figure 3.38: Visualization of vortex motion around oval slender structure

3.5.5 Flow characteristics and sand bed formation in flume

When the shear stress on the bed of an alluvial channel due to flowing of water is larger than the critical shear stress, the bed will become dynamic and will have a strong interaction with the flow. Depending on the flow, sediment and fluid characteristics, the bed will undergo different level of deformation and motion like ripples, dunes, anti-dunes etc. shown in figure 3.39. Schematic illustration of the scour hole development for pier and scour pattern are described in figure 3.40.

(a)

(b)

(c)

Figure 3.39: Scour pattern with mounds (a), depressions and ripples (b, c) at the end of the channel

3.5.6 Explanation on Development of scour hole

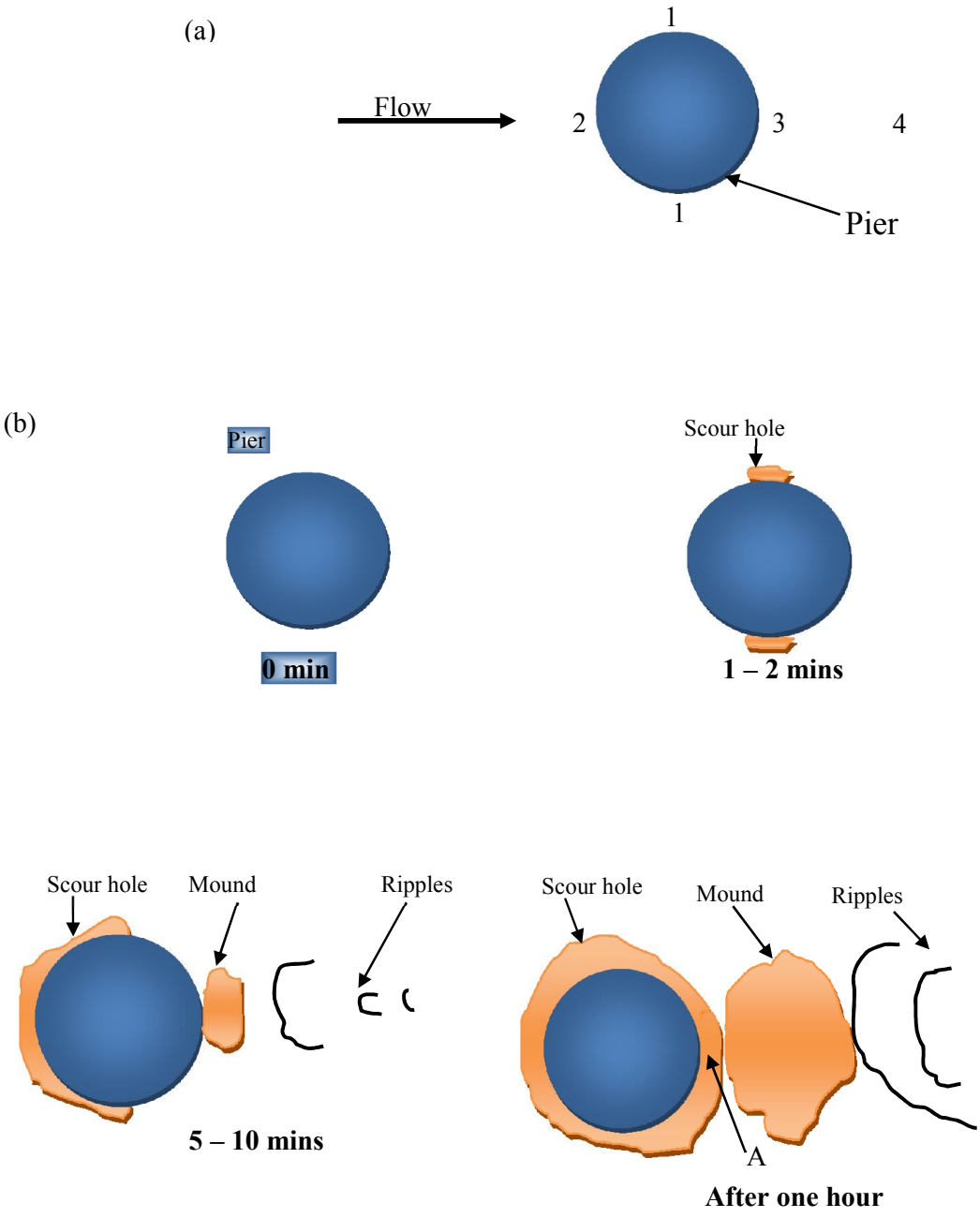

Figure 3.40: Schematic illustration of the scour hole development for the plain pier: (a) Scour pattern and (b) Sketches of the scour hole with time

3.6 Experimental study on scouring around pier model fitted with collar

Most common methods to prevent local scour around the pier consist in armoring devices of non-erodible bed, like the riprap, which can be in rock or artificial material. The present study intends to investigate a possible alternative to riprap as protection, a flow altering device called circular protective collar. The collar's efficiency in scour reduction was already investigated in past studies by many researchers. The collar placed at a low elevation relative to the bed is most effective to reduce the scour and possible combination of collar and slot may be more effective at reducing scour (Kumar et al 1999).

The growth of vortex can be arrested by retaining the vortex on a rigid surface such as collar and the efficiency of a collar is function of its width and vertical location (Singh et al 2001). Zarrati et al (2006) studied the use of independent and continuous pier collars in combination with riprap for reducing local scour around bridge pier groups. Their results showed that with two piers in line, a combination of continuous collars and riprap led to a scour reduction of about 50% and 60% for the front and rear piers, respectively.

Masjedi et al (2010) studied the use of oblong collars for reducing the effects of local scour at a bridge pier with the time aspect of the scour development. The time development of the local scour around the oblong pier fitted with and without collar plates was studied. Experiments were conducted for various size of rectangular collars fitted at the bed elevation on the scour depth at the circular pier with clear water scour condition. Dargahi (1990) has observed that, if the ratio of the collar thickness to the cylinder diameter becomes large, the effective pier diameter will increase, causing an increase in the scour depth.

In the present study, extensive experiments are carried out to predict the local scour around a circular pier in laboratory flume with and without collar plate. The collar plates are also circular in shape and placed concentrically with the cylindrical pier. The size of collar is kept two and three times of the cylindrical pier diameter. The effect of collar is studied for different discharge and Froude number. The maximum local scouring is measured and scour depth variation with time is presented.

3.6.1 Brief Description of experimental procedures

For experimental purpose, one cylindrical pier model of diameter 318 mm was used. One vertical scale was fitted with the model. The purpose of this scale around the pier was to facilitate the measurement of the magnitude of the scour depth by visualization from outside. In each case, the pier was placed on the centerline of the flume on sand bed. The collar used in the experiments was 5 mm thick and was made from a transparent acrylic material. Two different collar widths were used, with one having a width of two times the pier diameter (2D) while the other had a diameter of 3D, where D is the diameter of the pier. Figure 3.41 shows a pier fitted with a collar. For all of the tests with a collar, the collar was positioned at the bed level in accordance with the recommendations of earlier researchers (e.g., Ettema 1980; Kumar et al. 1999).

Figure 3.41: View of scour hole around circular pier fitted with collar

3.6.2 Test Program

The use of collars has been suggested as a possible pier scour mitigation technique by researchers, largely on the basis of model study results. The test program was developed to deal with the evaluation of the efficiency of using a collar as a mitigation technique against pier scour, with a major focus on the time required to achieve an equilibrium

scour condition. The test program was divided into three series of tests, with each test series representing a complete set of tests. The three series of tests are referred to as Series 1, Series 2, and Series 3. For all of the tests, the collar was positioned at the bed level. A summary of the basic test conditions and flow conditions is presented in Table 3.9.

Table 3.9: Summary of Test Program

Test	Discharge (lit/min)	Flow depth (mm)	Mean velocity (m/s)	Collar
Series 1	165	150	0.458	Without Collar
	210	180	0.486	
	260	190	0.570	
	305	220	0.578	
Series 2	155	145	0.389	With a collar of size 2D
	200	170	0.490	
	260	190	0. 570	
	300	230	0. 543	
Series 3	165	150	0.458	With a collar of size 3D
	220	190	0.482	
	270	200	0.562	
	310	235	0.549	

The first series of tests (Series 1) was designed to study the time development of scour as well as the efficacy of using a collar as a countermeasure for scour at a bridge pier. The first test under Series 1 tests was conducted without a collar fitted to the pier. In the second test series 2, a collar of width equal to two times the pier diameter was used. For both tests, a pier of diameter 318 mm was used. Tests were conducted under Series 1, namely: A test with a plain pier with varying discharge and the other one under Series 2 for a pier fitted with a 2D collar with varying discharge. Last one under Series 3 for a pier fitted with a 3D collar with varying discharge. The schematic diagram of collar fitted with pier is presented in Figure 3.42

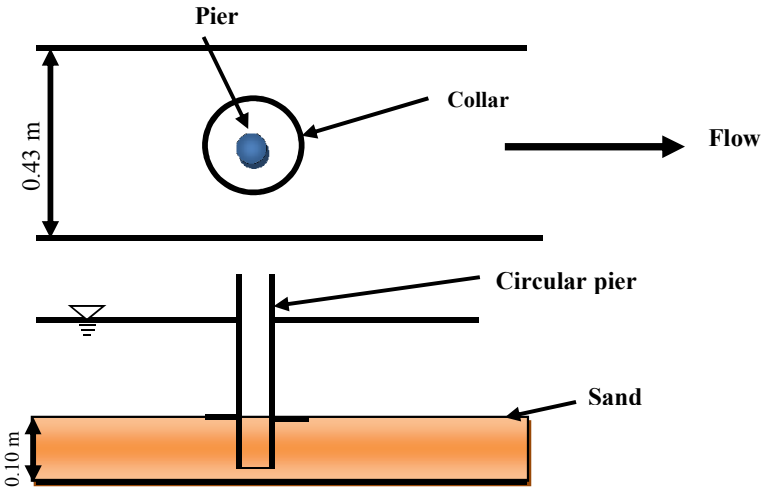

Figure 3.42: Schematic diagram of pier with collar

3.6.3 Effect of collar size on scouring

The non-dimensional scour depth is measured for different discharge and presented in the Figures 3.43 - 3.44. It is observed from the figure that scouring is decreased on addition of collar in the pier. The efficiency of collar to reduce the transient scouring is more. When the collar size is kept two times the pier diameter, it is observed less scour compared to no collar in the pier. Again it is observed that on using collar size three times the pier diameter, further scour hole depth is reduced. From this, one may infer that the using of collar is beneficiary to reduce the local scour depth around bridge pier.

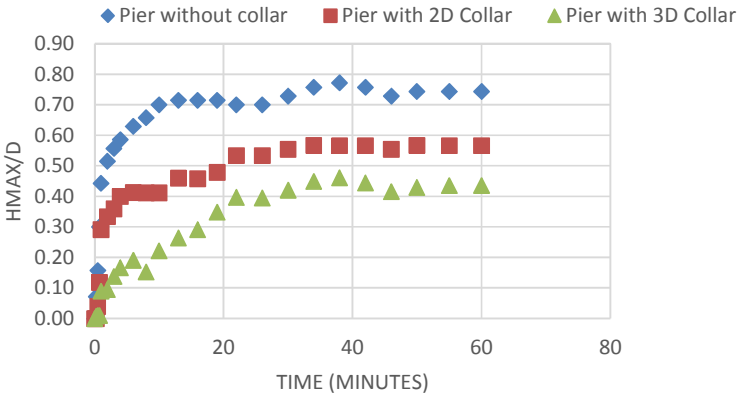

(a)Variation of maximum scour depth upstream of the pier for discharge 150 liter/min

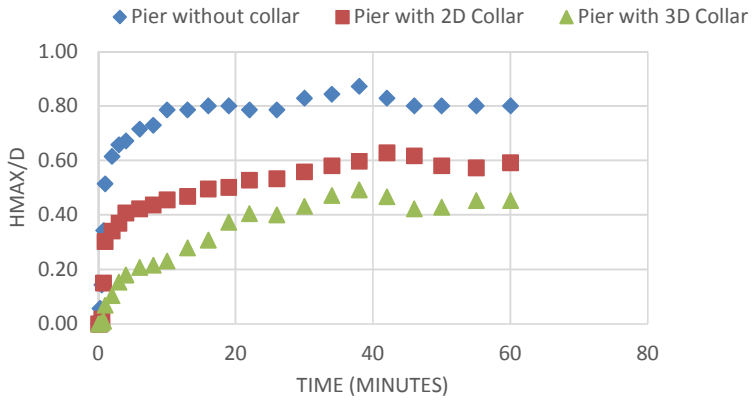

(b)Variation of maximum scour depth upstream of the pier for discharge 180 liter/min

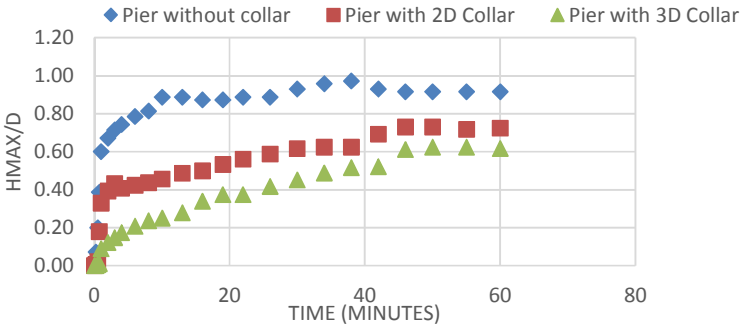

(c)Variation of maximum scour depth upstream of the pier for discharge 190 liter/min

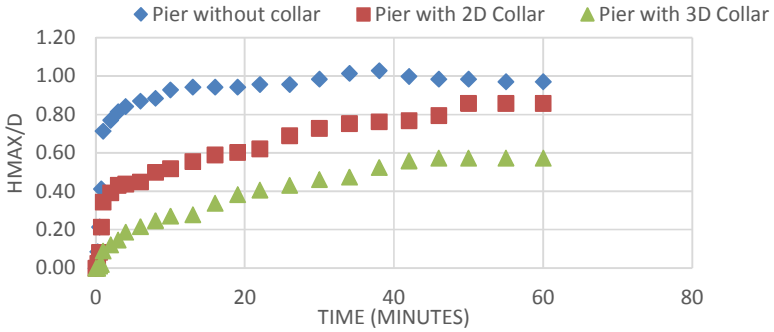

(d)Variation of maximum scour depth upstream of the pier for discharge 220 liter/min

Figure 3.43: Variation of maximum scour depth upstream of the pier for different discharges

The logarithmic variation of maximum scour depth around the pier with time is presented in Figure 3.44. It is observed from figure that the after, initially maximum scour occurs, then after the scour rate decreases. It is also observed that the scouring rate is dependent on discharge and depth of flow.

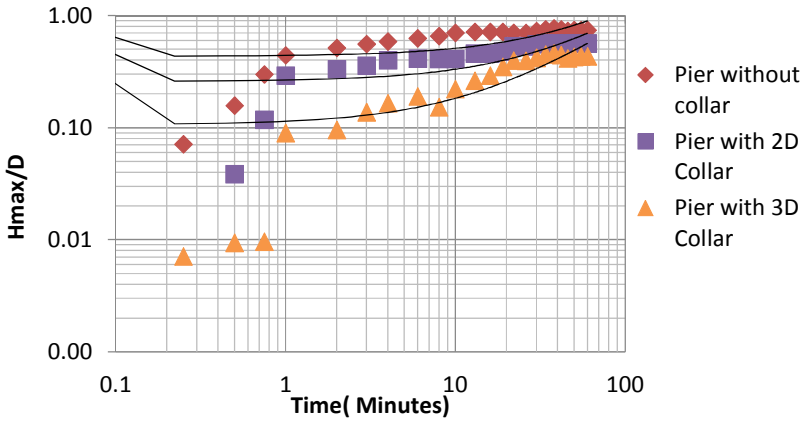

(a) Logarithmic Variation of maximum scour depth with time

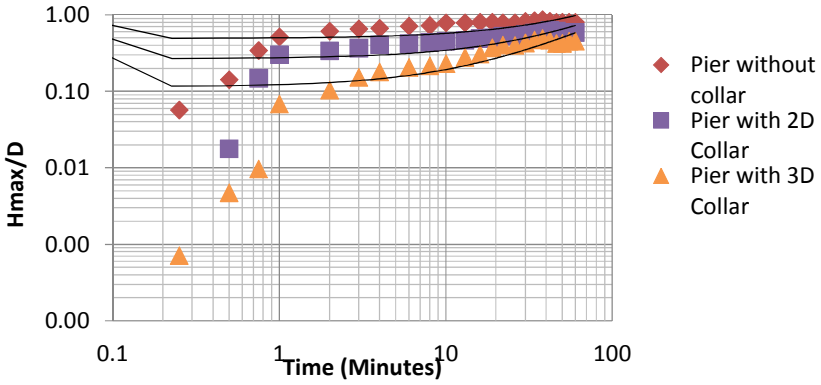

(b) Logarithmic Variation of maximum scour depth with time

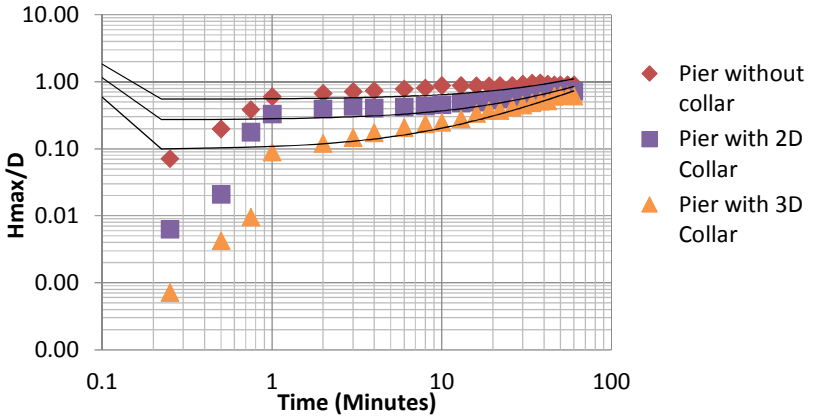

(c) Logarithmic Variation of maximum scour depth with time

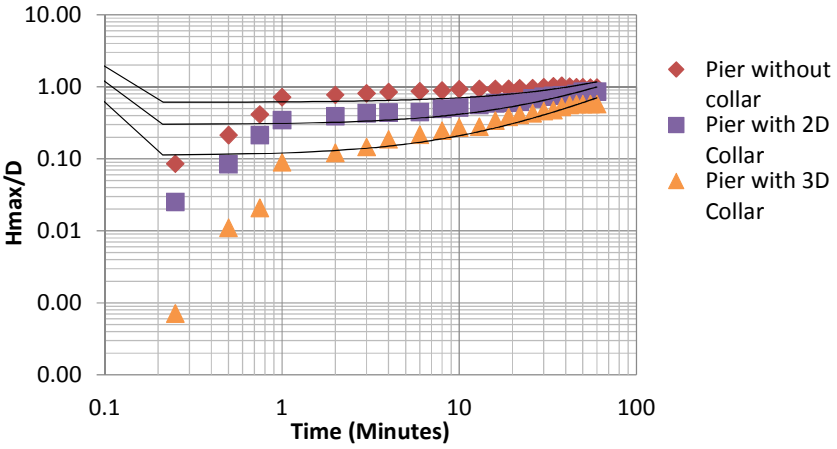

(d) Logarithmic Variation of maximum scour depth with time

Figure 3.44: Logarithmic Variation of maximum scour depth with time for different discharges

The experimental results signified that not only did the presence of collar reduce the scour depth; it also shows the rate of temporal development of the scour hole was also reduced. Figure 3.45 shows the scouring condition of the case of pier fitted with a collar and without collar. This pictorial view is taken at similar boundary condition of the flow conditions.

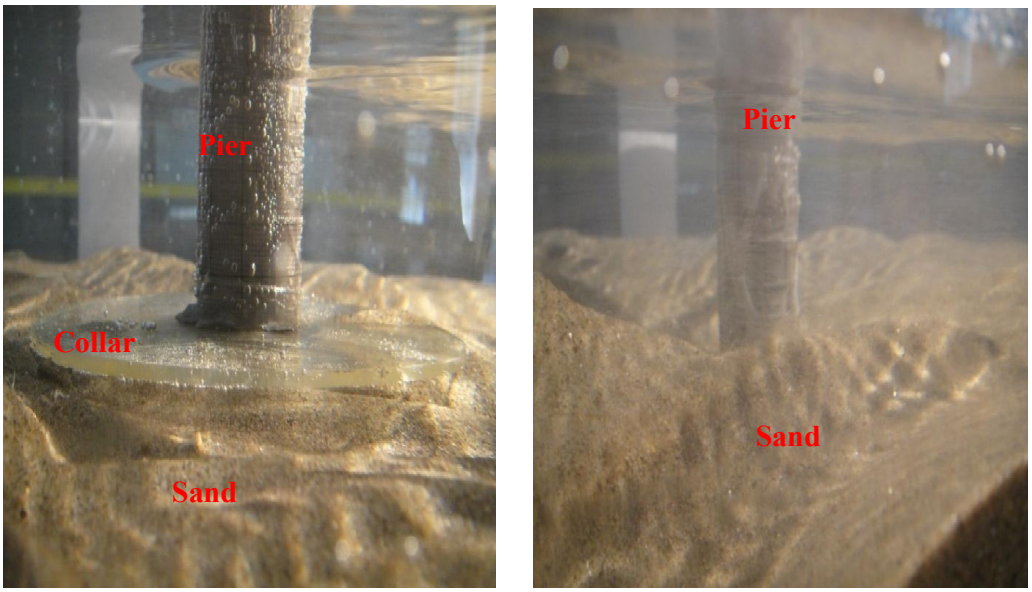

(a) (b)

Figure 3.45: Experimental picture of (a) a pier fitted with collar (b) a pier without collar

3.6.4 Explanation on Development of scour hole with collar

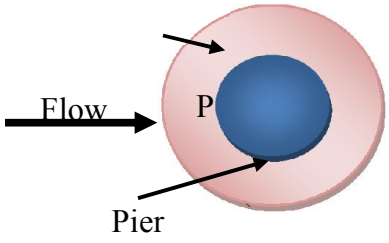

(a) Schematic diagram of Pier

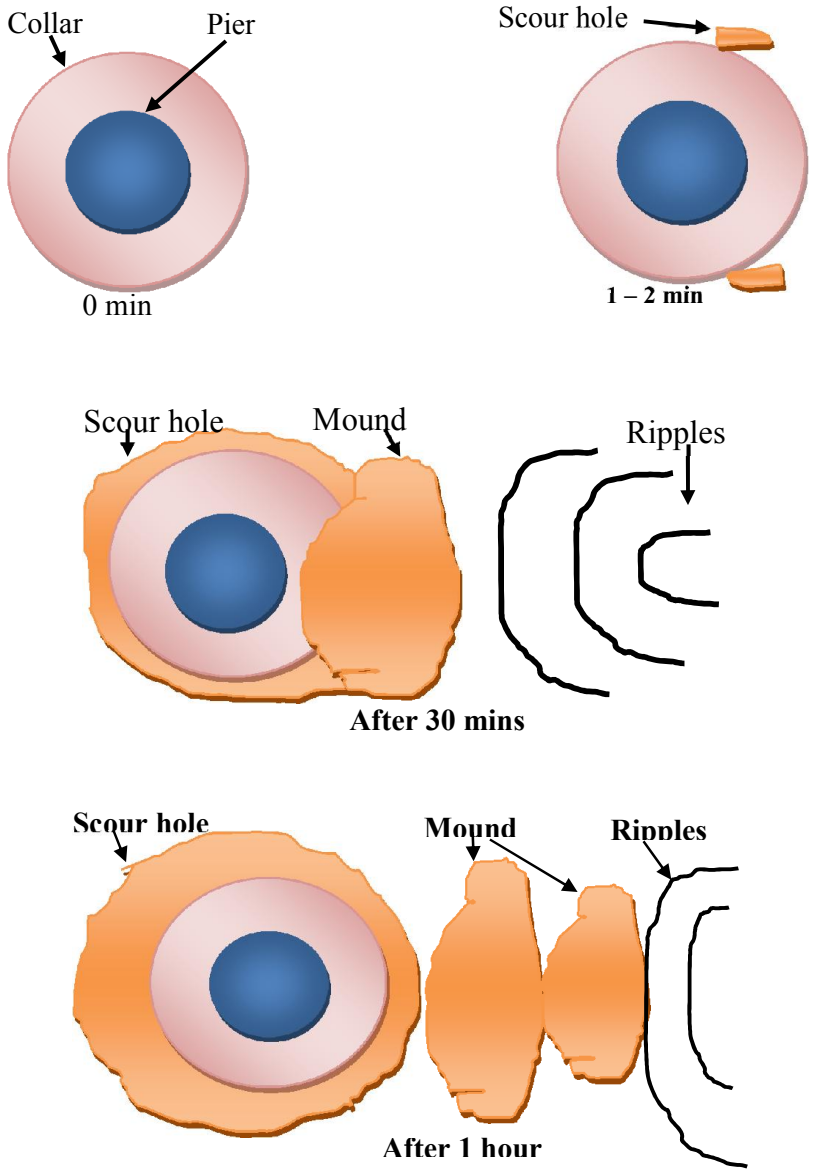

(b): Schematic diagram of development of scour hole with time

Figure 3.46: Schematic diagram of development of scour hole with time (a & b)

The local scour that takes place around the piers mounted on an erodible bed is a complex phenomenon. The depth of scour hole around pier depends on pier size and shape and different flow parameters. Due to formation of vortex around the pier, the flow patter

changes around the structure as a consequent the flow energy changes. The change of flow energy enhances erosion and deposition of sand particles surrounding the obstructions. Schematic diagram of development of scour hole with time fitted with collar in mention in figure 3.46. Again as the change of bed geometry changes due to scouring, the flow behavior becomes complex one. The attempt has been made in this study to observe the flow characteristics and maximum scour hole around pier with collar fitted with pier. Comparative analysis revealed that pier fitted with collar reduces the temporal scouring effect. The maximum efficiency is observed when the collar size is three times the pier diameter. Bigger size collar is impractical and may reverse effect the scouring. In bridge pier construction, the collar may be used for reducing the scouring effect. The fluid-structure interaction force on concentric collar is very complex and the design of collar needs special attention during its construction.